ISSN 0023-1584, Kinetics and Catalysis, 2018, Vol. 59, No. 1, pp. 23–47. © Pleiades Publishing, Ltd., 2018.
Original Russian Text © A.S. Chikunov, O.P. Taran, A.A. Shubin, I.L. Zilberberg, V.N. Parmon, 2018, published in Kinetika i Kataliz, 2018, Vol. 59, No. 1, pp. 29–56.

Oxidation of Water to Molecular Oxygen by One-Electron Oxidants on Transition Metal Hydroxides[1]

A. S. Chikunov[a], O. P. Taran[a, b, *], A. A. Shubin[a, c], I. L. Zilberberg[a, c], and V. N. Parmon[a, c]

[a] *Boreskov Institute of Catalysis, Siberian Branch, Russian Academy of Sciences, Novosibirsk, 630090 Russia*
[b] *Novosibirsk State Technical University, Novosibirsk, 630073 Russia*
[c] *Novosibirsk State University, Novosibirsk, 630090 Russia*
**e-mail: oxanap@catalysis.ru*

Received May 11, 2017

Abstract—Surveyed in this review are the most important achievements in the research and development of catalysts based on Mn, Fe, Co, and Cu hydroxides for the oxidation of water to molecular oxygen by chemical oxidizing agents obtained, for the most part, at Boreskov Institute of Catalysis, Siberian Branch of the Russian Academy of Sciences. An analysis of the results of kinetic studies on water oxidation in the presence of the above-menthioned catalysts together with data obtained by quantum chemistry methods allowed us to make a conclusion on the general nature and process mechanism both in the presence of artificial catalytic systems based on metal hydroxides and the natural enzyme photosystem II of green plants. The most important properties of hydroxo compounds responsible for catalytic activity in the oxidation of water by one-electron oxidants are discussed, and a possible reaction mechanism is considered.

Keywords: water oxidation, one-electron oxidants, artificial catalytic systems, transition metal hydroxides, natural enzyme photosystem II, catalytic activity of hydroxo compounds, artificial photosynthesis, oxygen evolution

DOI: 10.1134/S0023158418010032

INTRODUCTION

The energy crisis in the early 1970s initiated intensive studies oriented to the development of alternative and renewable energy sources. Special attention was paid to the conversion and storage of solar energy, whose attractiveness is explained by its inexhaustibility and enormous potential. More than 2.2×10^{24} J of this energy arrives at the Earth's surface for one year [1]. Although energy assimilated as a result of natural photosynthesis in the biosphere is lower by five orders of magnitude, the quantity of energy accumulated in the products of photosynthesis is much higher than the annual energy requirement of humanity and comparable with the total potential of the overall proved reserves of traditional fossil fuels [2].

Among possible approaches to the use of solar energy, such as its conversion into thermal energy by the concentration of a solar radiation flux or direct transformation into electricity with the aid of solar batteries, the possibility of artificially reproducing natural photosynthesis has been an area of special interest since forever. Attention to the artificial photosynthesizing systems, in which the quantum processes of radiant energy conversion are implemented, is related to the possibility of energy storage in the most convenient form as chemical compounds.

Natural photosynthesis occurs under the action of visible radiation, and it is a complex process, which can be reduced, as a rule, to the synthesis of carbohydrates as a result of light-stimulated electron transfer from a donor molecule in the environment to the molecule of carbon dioxide (or another substrate) in the course of the subsequent dark stages. Microorganisms performed the most primitive natural photosynthesis billions years ago, and it has continued to this day. In the simplest photosynthesizing microorganisms like archaebacteria, purple and green bacteria, and halobacteria, Fe^{2+}_{aq}, H_2, H_2S, SO_4^{2-}, RR'CHOH, etc., serve as electron donors (Fig. 1a). Approximately 3.5 billion years ago, the subsequent evolution of the biosphere led to the appearance of a new kind of microorganisms—cyanobacteria or blue-green algae, which are capable of using water molecules as an electron donor to oxidize water to molecular oxygen (Fig. 1b). These microorganisms are responsible for the conversion of the reducing atmosphere of the Earth into the oxidizing one, which resulted in the occurrence of the contemporary forms of aerobic metabolism and the for-

[1] This paper is based on materials presented at the X International Conference "Mechanisms of Catalytic Reactions" (October 2–6, 2016, Svetlogorsk).

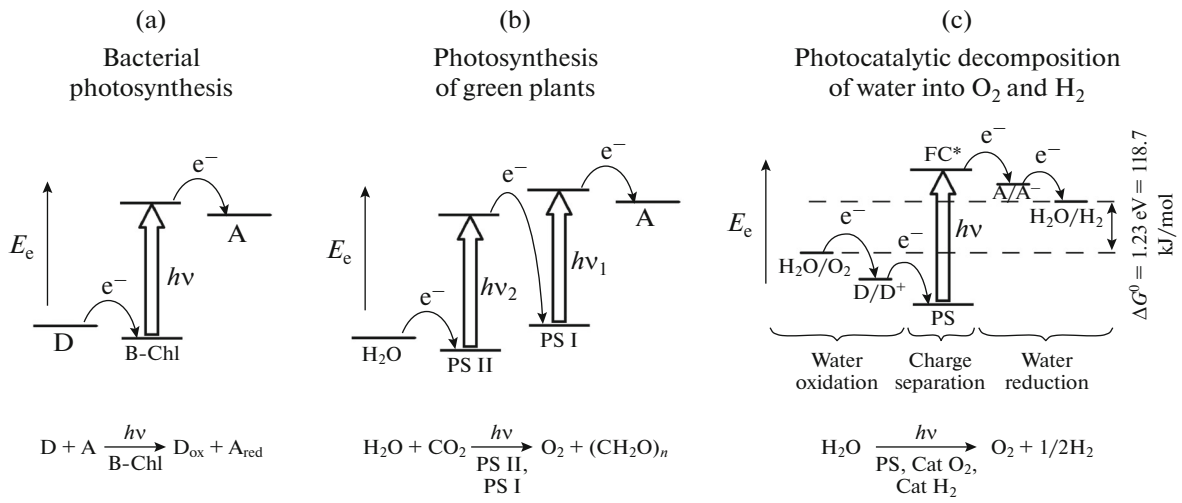

Fig. 1. Schematic diagrams of electron transfer in natural and artificial photocatalytic systems: (a) bacterial photosynthesis, where B-Chl is bacteriochlorophyll, D is an electron donor (Fe^{2+}_{aq}, H_2, H_2S, RR'CHOH, etc.), and A is the final acceptor (NADH, ATP); (b) photosynthesis of green plants; and (c) artificial photocatalytic system for the complete decomposition of water into hydrogen and oxygen, where Cat_{O_2} and Cat_{H_2} are the catalysts of water oxidation and reduction, respectively; PS is a photocatalyst responsible for the photoinitiated charge separation and transfer from Cat_{O_2} to Cat_{H_2}; D and A are the intermediate electron donor and acceptor, respectively; and E_e is the electron energy.

mation of the multicellular forms of life. Green plants, which appeared much more recently, became the heirs of cyanobacteria or blue-green algae; the oxidation of water to oxygen also occurs in the photosynthesis of green plants.

At present, it is universally recognized that the microorganisms capable of oxidizing water appeared as a result of the strong and genetically fixed symbiosis of photosynthesizing protozoan microorganisms, which use the above compounds as a primary donor, and other photosynthesizing microorganisms with unstable genetic apparatus, which were not completely identified still; nevertheless, these latter possess an enormous evolutionary advantage—the ability to use the molecules of water (the most common compound) as an accessible electron donor [3]. Since the natural evolutionary selection require the simultaneous appearance of an acquired character and the possibility of its genetic fixation and the subsequent optimization, one should assume that the ancestors of these unidentified organisms that oxidize water could bind some compounds (which are capable of oxidizing water and became the basis of a prosthetic groups of the subsequently optimized enzymes of corresponding microorganisms) from the aquatic environment (simply speaking, from a puddle). Our experience in the development of artificial catalysts for water oxidation showed that, undoubtedly, these prototypes were the small clusters of hydroxides of a number of common transition metals, primarily, manganese, iron, and copper, which usually available in natural water. The general reaction scheme of natural photosynthesis in green plants is usually described by the simple overall reaction

$$6H_2O + 6CO_2 \xrightarrow{h\nu} (CH_2O)_6 + 6O_2\uparrow. \qquad (I)$$

The possibility of photo-initiated charge separation with the subsequent electron transfer via complex transport chains is ensured by two photosystems immobilized on the thylakoid membrane of chloroplasts. Photosystem I reproduces the function of bacterial photosynthesis, and it is responsible for the reduction of carbon dioxide and the synthesis of carbohydrates, whereas photosystem II generates intermediate electron donors necessary for photosystem I by the four-electron oxidation of water to molecular oxygen.

From the point of view of artificial photosynthesis, which can ensure the conversion of solar energy into the energy of chemical fuel, a simpler system in which the following overall reaction of the complete decomposition of water into hydrogen and oxygen occurs under the action of visible light (Fig. 1c) is of the greatest interest:

$$H_2O \xrightarrow{h\nu} H_2\uparrow + 0.5O_2\uparrow. \qquad (II)$$

The process of water photodecomposition includes three basic stages. At the first stage, the absorption of a light quantum by a photocatalyst with the subsequent charge separation occurs:

$$D + A \xrightarrow{h\nu} D^+ + A^-, \qquad (III)$$

where D is a primary electron donor, and A is an acceptor.

The dark stages follow the stage of charge separation: the oxidation of water to molecular oxygen

$$2H_2O - 4e^- \rightarrow 4H^+ + O_2\uparrow \quad \text{(IV)}$$

and, finally, the reduction of water to hydrogen

$$2H_2O + 2e^- \rightarrow H_2\uparrow + 2OH^-. \quad \text{(V)}$$

From the point of view of energy storage and the production of hydrogen like environmentally-friendly fuel, reaction (V) of the two-electron reduction of water to H_2 is a target stage, which, undoubtedly, requires special catalysts. However, the stage of water oxidation with the simultaneous transfer of four electrons is most difficult to perform.

The photocatalysts utilized at stage (III) in the molecular photocatalytic systems, which absorb a light quantum to be converted into an excited state, are capable of generating only one-electron reducing and oxidizing agents (A^- and D^+, respectively). Therefore, a catalyst is required for the water oxidation stage, which is capable of accumulating four oxidative equivalents for successive one-electron events. This dimmer are able to generate a primary oxidizing agent under the irradiance of light with wavelength less than 680 nm this oxidizing agent has a formal electrochemical potential of +1.3 V relative to the normal hydrogen electrode (NHE) [4].

In numerous research works dedicated to the development of molecular photocatalytic systems for water splitting, it was established that the closest artificial analog of natural chlorophyll is the complex of trisbipyridyl ruthenium(II) $Ru(bpy)_3^{2+}$ (where bpy is 2',2-dipyridyl) and analogous complexes like ML_3^{3+}, where M is a metal atom (for example, Ru, Ir, Fe, Os, etc.), and L is a ligand like bipyridyl, phenanthroline, bipyrimidine, etc. Under the action of visible light with a wavelength of 420–520 nm, this metal-containing complex in the presence of specially chosen electron acceptors can generate a primary one-electron oxidizing agent, which also possesses a high oxidation potential (+1.27 V relative to NHE) sufficient for oxidation of water over a wide range of pH from 0.5 to 14. For example, in the presence of persulfate as a primary electron acceptor, the following irreversible reaction occurs under the action of visible light:

$$Ru(bpy)_3^{2+} + S_2O_8^{2-} \xrightarrow{h\nu} Ru(bpy)_3^{3+} + 2SO_4^{2-}. \quad \text{(VI)}$$

The so-called oxygen-releasing complex of photosystem II serves as a catalyst, which accumulates four oxidizing equivalents, in natural photosynthesis. According to available data, the prosthetic group of the oxygen-releasing complex contains four manganese ions, one calcium atom, and five oxygen atoms. The $CaMn_4O_5$ cluster resembles a distorted chair with the seat in shape, so-called cubane in which the seat is formed by three manganese atoms, four oxygen atoms, and a calcium atom and the back of the chair, by distant manganese and oxygen atoms [5]. It was established that the oxygen-releasing complex can take five successive states (S_0, S_1, S_2, S_3, and S_4), which differ in the degree of oxidation of the prosthetic group and follow each other on the consecutive one-electron oxidation of the oxygen-releasing complex in the sum of 1, 2, 3, and 4 electrons, respectively. Transitions between some states are accompanied by the release of protons [6]:

$$2H_2O \rightarrow S_0 \xrightarrow{-H^+,-e^-} S_1 \xrightarrow{-e^-} S_2 \xrightarrow{-H^+,-e^-} S_3 \xrightarrow{-2H^+,-e^-} S_4 \rightarrow O_2 + H^+ \quad \text{(VII)}$$

The oxygen-releasing complex in the states S_0 and S_1 is stable in the darkness, whereas it is spontaneously reduced to S_1 in the states S_2 and S_3. The photosystem II adapted to the darkness contains a mixture of oxygen-releasing complexes in the states S_0 (25%) and S_1 (75%). In the state S_4, the complex is unstable, and it is spontaneously converted into S_0 within a time of about 1.1 ms with the liberation of an oxygen molecule [7].

The intensive search for and study of the mechanism of action of artificial catalysts (the analogs of oxygen-releasing complexes) for the oxidation of water with chemical compounds (one-electron oxidizing agents) under mild conditions are active up to the present. A considerable number of experimental and theoretical (quantum-chemical) studies in this area have been performed at the Boreskov Institute of Catalysis, Siberian Branch of the Russian Academy of Sciences. Considerable progress has been made toward the selection of both catalysts and one-electron oxidizing agents for the oxidation of water [8–12].

The catalysts proposed can be tentatively divided into two groups. The first group contains heterogeneous and microheterogeneous catalysts, which include the massive oxides of noble metals (ruthenium, platinum, iridium) or those supported onto oxide carriers, manganese dioxide, and the hydroxides of iron, cobalt, nickel, and copper. Colloidal catalysts based on RuO_2 (RuO_2/TiO_2) stabilized by polyvinyl alcohol and starch and the hydroxides of Mn, Cu, Fe, and Co immobilized on lipid vesicle membranes can also be attributed to this group. The colloidal hydroxides of a number of metals also belong to the microheterogeneous systems; with the use of the aqua cations Co^{2+} as an example, it was demonstrated that these

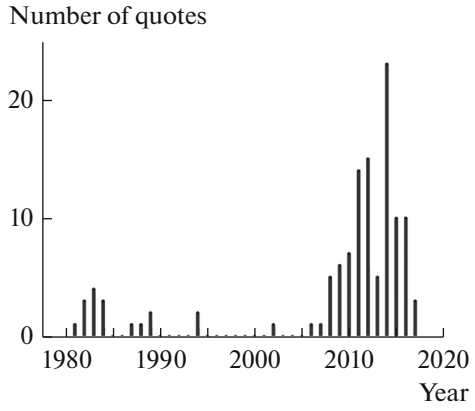

Fig. 2. Dynamics of the quoting of publications [20–22] dedicated to the development of photocatalytic systems for the oxidation of water to oxygen at the Boreskov Institute of Catalysis, Siberian Branch of the Russian Academy of Sciences (according to the data of Scopus.com).

hydroxides are formed from initially water-soluble aqua cations directly in the course of the catalytic oxidation of water.

The second group contains homogeneous catalysts including metal complex catalysts—primarily, bi- and tetranuclear complexes of ruthenium, manganese, and cobalt with nitrogen-containing ligands. There are published data on the catalysis of a water oxidation reaction by mononuclear complexes [11, 13]. However, in this case, a substantial portion of the initial complex compound is destroyed in the course of reaction and form dimeric or even polymeric μ forms with bridging oxo/hydroxo groups, which finally serve as a catalyst. (The compounds in which metal ions are bound through bridging atoms, in this case, through oxygen, are referred to as μ forms.) Note that, in the vast body of researches dedicated to metal complex catalysts with two, three, and four metal atoms, the possible participation of the hydrolyzed polynuclear forms of complexes in the catalytic cycle of water oxidation was not examined. Moreover, there is direct evidence of the destruction of a substantial portion of the initial binuclear complex compound to corresponding oxide hydroxides [14]. Finally, recent publications [13, 15–18] reported on the inorganic polyoxometalate complex $[Ru_4(\mu\text{-}O)_4(\mu\text{-}OH)_2(H_2O)_4(\gamma\text{-}SiW_{10}O_{36})_2]^{10-}$, which contains the catalytically active tetra-Ru(IV)oxo group stabilized by a polyoxometalate environment. This active center has oxo hydroxide nature, and the complex itself was found an effective and stable catalyst for the oxidation of water with the measured maximum turnover number TON ≈ 500 [19].

Despite the successes achieved in the 1970–1980s, the intensity of studies directed toward the development of artificial photosynthesis and, in particular, catalytic systems for water oxidation, gradually decreased and they almost ceased in the late 1990s. However, interest in this problem has resumed in the middle 2000s. This time, a desire to solve the environmental problems of power engineering rather than a sequential increase in the prices of traditional fossil fuels was the main stimulus to search for the molecular photocatalytic systems of water decomposition. As a result, attention was focused on the studies of the catalytic oxidation of water performed in the 1980–1990s. If we trace the dynamics of quoting three best known publications on the development of molecular photocatalytic systems for the decomposition of water at the Boreskov Institute of Catalysis, Siberian Branch of the Russian Academy of Sciences [20–22], we can see a noticeable increase in the number of their citations starting in 2006–2008 (Fig. 2).

Thus, it is reasonable to generalize the results obtained at this institute in the research and development of catalysts based on transition metal hydroxides for the oxidation of water. We believe that this generalization will make it possible not only to demonstrate the advances of the institute in the solution of the discussed problem but also to develop a program for the subsequent basic research in this undoubtedly important area.

STUDY OF THE CATALYTIC ACTIVITY OF COMPLEXES CONTAINING TRANSITION METAL ATOMS

Early in the development of artificial photosynthesis systems, attention was focused on the creation of homogeneous catalytic systems capable of oxidizing water to molecular oxygen (similarly to the natural oxygen-releasing complex of photosystem II) under the action of sufficiently strong one-electron oxidizing agents D^+ ($Ru(bpy)_3^{3+}$, Ce_{aq}^{4+}, and MnO_4^-). Metal phthalocyanines were considered as the most promising homogeneous catalysts [20] because they are structurally similar to bacteriochlorophylls. In the one-electron oxidation of metal phthalocyanines, the electron can be removed either from a metal ion (this is characteristic of the complexes of Co, Fe, and Mn) or from a cyclic macroligand (this is characteristic of the tetrapyrrole complexes of Cu, Cr, Zn, etc.), and the former process occurs at lower oxidation potentials than the latter. The occurrence of two parallel oxidation–reduction processes leads to the fact that the yield of oxygen becomes lower that that expected according to the stoichiometry of the reaction

$$4D^+ + 2H_2O \xrightarrow[\text{Cat.}]{} 4D + O_2 + 4H^+. \qquad \text{(VIII)}$$

Of course, the undesirable oxidation of organic ligands in the active center of the catalyst decreases the yield of oxygen as the target product. For this reason, the yield of molecular oxygen on a consumed oxidant basis (S_{O_2}) rather than activity is considered the main parameter responsible for the quality of catalyst. Reaction (VIII) is pH-dependent, and an oxidant with

the apparent electrode potential $S_E = +0.82$ V relative to NHE at pH 7.0 is required for its occurrence.

It was assumed that the stability of macroligands to oxidation could be increased by the introduction of electrophilic substituents into them. For this purpose, the catalytic action of the sulfonated phthalocyanines of Cr, Mn, Ni, Cu, Zn, Fe, and Co and Co tetra(sulfophenyl)porphin in the reaction of water oxidation by the complex $Ru(bpy)_3^{3+}$ was studied. Elizarova et al. [20] found that Cr-, Mn-, and Al-containing phthalocyanines are decomposed under the action of an oxidant to form the catalytically inactive solutions of the aquated ions of corresponding metals. The tetrasulfophthalocyanines of Co and Fe exhibited the greatest activity in reaction (VIII) at pH 9.2 (S_{O_2} = 50 and 47%, respectively). The Co tetra(sulfophenyl)porphin was found similar in its catalytic properties to phthalocyanines (S_{O_2} = 65%). The effect of chemically different substituents introduced into the structure of a tetrapyrrole macroligand on the yield of oxygen was studied on the basis of an example of cobalt tetrasulfophthalocyanine. The introduction of a weak-acceptor bromine substituent increased the yield of O_2 to 62%. The introduction of a strong acceptor group ($-NO_2$) led to a similar result (S_{O_2} = 65%). At the same time, the donor OH group sharply decreased S_{O_2} (to 24%), and the amino group, on the contrary, increased the yield of oxygen to 54%. Thus, the influence of a substituent on the catalytic properties of phthalocyanines was found to be much more intricate and significant than it was assumed previously.

Parmon et al. [23] measured the electrochemical potentials (E) of highly acidic (pH 1.3) dilute aqueous solutions of a large number of metal phthalocyanines (10^{-5}–10^{-4} mol/L) at metal phthalocyanine : oxidant ($KMnO_4$ and/or $Ce(SO_4)_2$) molar ratios from 0.1 to 1. They found that the slopes of straight lines in the E_{mes}–log (oxidant/catalyst) coordinates in a reaction with the participation of Co complexes are ~80 mV, which is characteristic of irreversible processes, instead of expected 9 mV inherent in reversible one-electron processes. Because the initial complexes of metal phthalocyanines are completely dimerized under the conditions of measurements, it was hypothesized that the irreversibility was caused by the slow degradation of the initial dimeric compounds and the possible polymerization of their oxidation products. The occurrence of these processes was not demonstrated by potentiometric titration because of the strong adsorption of phthalocyanines on the surface of electrodes. However, an analysis of the optical absorption spectra of metal phthalocyanine solutions on their titration with an oxidant made it possible to confirm that both of the processes really occurred [23]. Thus, it was possible to distinguish between the oxidation of a metal cation and the oxidation of a macroligand because the oxidation of a metal does not disturb the chain of conjugated bonds responsible for an intense color of the complexes. For example, after the addition of an oxidant (Ce^{4+} or MnO_4^-) to Co(II) tetrasulfophthalocyanine in a molar ratio of no higher than 1 : 1, rapid transformations with rate constants higher than 10^4 L mol^{-1} s^{-1}, which are characteristic of rapid bimolecular reactions, were observed in the spectrum. In this case, a new absorption maximum at 14800 cm^{-1} appeared in the spectrum of the initial solution in place of maximums at 15900 and 15200 cm^{-1} (metal–ligand charge transfer bands). A similar change in the spectrum, which was observed on the storage of Co(II) tetrasulfophthalocyanine in air, made it possible to attribute it to a transition of the metal atom to a more oxidized state, i.e., to Co(III). The further addition of the oxidant led to the discoloration of solutions, that is, to a decrease in the absorption intensity of the Co(III) complex without a distortion in the shape of the spectrum, which is, obviously, related to the oxidation of the macroligand. At the molar ratio oxidant : catalyst = 1.5 : 1 (which is clearly insufficient for the one-electron oxidation of each macroligand), only 15–20% of the initial metal complex remained in the solution. This can be explained by the fact that the oxidation of even one macroligand leads to the disturbance of the chain of conjugated bonds in the entire dimeric complex. On the addition of an oxidant in small amounts to Co(II) disulfophthalocyanine, the complexes of Co(III) are not formed and the solution is immediately discolored. At the same time, an increase in the concentration of Co(III) was observed as the oxidant concentration in the solution of Co(II) disulfobromophthalocyanine was increased to reach the molar ratio catalyst : oxidant = 1 : 1, and discoloration occurred only with a large molar excess of the oxidant (3 : 1). Thus, Parmon et al. [23] found that the introduction of a weak electron acceptor such as bromine considerably increases the stability of the macroligand to oxidation. The stability of complexes increases many times upon the introduction of a strong acceptor (like the nitro group). In this case, at the molar ratio oxidant : catalyst = 2 : 1, the optical absorption spectrum did not undergo noticeable changes even after 30 min. A more complicated picture was observed in the spectra of complexes containing Cu^{2+} and Fe^{3+} ions. Under the action of an oxidant, Cu(II) disulfophthalocyanine rapidly decolorized; moreover, the observed effect was accompanied by the formation of a short-lived bright violet intermediate. Upon the addition of an oxidant to iron tetrasulfophthalocyanine in a molar ratio of 0.5 : 1, the initial absorption band intensity sharply decreased and the intensity of another band attributed to the resulting intermediate increased. On the aging of a solution for several ten minutes, the intensity of the latter decreased and the intensity of a band due to the initial compound decreased. The phenomena described can be explained by the reversible processes of the conver-

sion of metal complex catalysts including those related to the oxidation of macroligands.

An EPR study of the freshly prepared unoxidized Co(II) tetrasulfophthalocyanine complex in a 5 M solution of H_2SO_4 frozen at 77 K revealed the presence of a clear but strongly broadened (ΔH_{max} = 370 Oe) signal with $g = 2.27 \pm 0.02$, which corresponds to an isolated mononuclear complex [23]. The same complex in a 0.05 M solution of H_2SO_4 did not give such a signal; however, in this case, a signal in the half field ($g > 4$) and a trace signal with $g < 2$ attributed to the di- or polymeric forms of the initial complexes, respectively, appeared. All of the signals disappeared upon the addition of oxidizing agents.

Thus, metal phthalocyanines and metal porphyrins (where the metals are Mn, Fe, Co, and Cu) are capable of catalyzing the oxidation of water to molecular oxygen with one-electron oxidizing agents at neutral and alkaline values of pH. In this case, the processes of both the reversible and irreversible dimerization, polymerization, and disproportionation of metal phthalocyanines exert a considerable effect on the oxidation of metal phthalocyanines in dilute solutions, which is necessary for the occurrence of reaction (VIII) and, therefore, on their catalytic properties. In the case of Co(II), the coordinated metal ions are oxidized more rapidly than macroligands, and the strong interaction between metal phthalocyanines in the polymeric forms can lead to a disturbance in the conjugated bonds of macroligands even in the one-electron oxidation only of one of them.

CATALYTIC PROPERTIES OF TRANSITION METAL HYDROXIDES ON SOLID SUPPORTS

At the initial stage of the development of the molecular systems of artificial photosynthesis, primary attention was focused on a study of chemically obtained strong one-electron oxidants capable of oxidizing water to molecular oxygen in the absence of both light and additional catalysts [24]. Among these oxidants are the diimine complexes of iron(III) and ruthenium(III) with the general formula ML_3^{3+}, where L is 1,10-phenanthroline (phen) or 2,2'-bipyridyl (bpy). The standard electrode potentials of these complexes for the pair RuL_3^{3+}/RuL_3^{2+} are 1.22 and 1.27 V relative to NHE with L = phen and bpy, respectively, or 1.11 and 1.07 V, respectively, for the pair FeL_3^{3+}/FeL_3^{2+} [25]. It was found that the release of oxygen from the solutions of the above oxidants occurs only in an alkaline reaction medium; in this case, the aging of a solution of $Fe(bpy)_3^{3+}$ at pH 9.2 for 30 min led to an increase in the yield of oxygen. The release of oxygen decreased in the course of aging. With the use of UV–Vis spectroscopy, it was demonstrated that, after solution aging for 30 min, only 80–90% of the initial amount of $Fe(bpy)_3^{3+}$ remained in the solution, and from 2 to 8% of the $Fe(bpy)_3^{2+}$ reduced species was accumulated. Because the aging of Fe(III) metal complexes in the alkaline solutions leads to their hydrolysis, it was assumed that the hydrolyzed portion of the complex serves as a catalyst. To test this hypothesis, experiments were carried out in which the release of oxygen from water occurred under the action of $Fe(bpy)_3^{3+}$ in the presence of HCl, $FeCl_3$, and $CoCl_3$. In the presence of HCl, oxygen was not released even under the conditions of solution aging. On the contrary, the addition of iron and cobalt chlorides increased the yield of oxygen.

Elizarova et al. [21] studied the oxidation of water by the $Ru(bpy)_3^{3+}$ complex in a batch reactor at the initial values of pH 6 and 10 in the presence of the dipyridyl compounds of Co(II), Co(III), Cu(II), and Fe(III) and the complexes of cobalt(III) with ammonia, ethylenediamine, and hydroxy acids. Table 1 indicates that the initial value of pH in reaction solution exerts a considerable effect on the yield of oxygen. This is a consequence of not only a change in the potential necessary for water oxidation according to reaction (VIII) but also an increase in the degrees of conversion of the hydrolysis and oxolation of the initial metal complexes. In this case, the nature of ligands in the initial complexes plays an important role because the ligands are responsible for the final characteristics of the products of hydrolysis.

For testing the hypothesis that the products of partial hydrolysis are responsible for the catalytic activity of the complex compounds of transition metals, Elizarova et al. [21] studied the effect of the nature of ligands and the coordination saturation of complexes on catalytic properties. It is well known that the lower the coordination saturation of complex compounds, the easier their hydrolysis. The compounds of Co(II) with hydroxy acids in a molar ratio of 1 : 1 exhibited high catalytic activity, whereas more highly coordinated compounds were formed in the absence of hydroxy acids; because of this, the yield of oxygen decreased. In the series of the ammonium complexes of Co(III), a minimum yield of oxygen was observed in the presence of coordinatively saturated $Co(NH_3)_6^{3+}$, and a maximum yield, in the presence of the most unsaturated complex *cis*-$Co(NH_3)_4(H_2O)_2^{3+}$. The trisbipyridyl complex of cobalt(III) also exhibited sufficiently high selectivity; however, it also underwent partial hydrolysis in solutions with pH 10, as evidenced by a significant change in the optical absorption spectrum (an absorption band at 33000 cm^{-1}, which was observed in solutions with pH 1, disappeared at pH 10, and only an absorption band at 32000 cm^{-1} remained). A comparison between the catalytic properties of $FeCl_3$ and the $[Fe_2O(phen)_4]Cl_4$ complex made it possible to draw the conclusion that the formation of μ-oxo bridging

bonds between metal ions exerts a considerable effect on the efficiency of catalysts. Based on the above results, concluded that the products of the partial hydrolysis of metal-containing precursor compounds are the true catalysts of water oxidation in the presence of strong one-electron oxidants. Therefore, the subsequent studies were oriented toward the development of catalytic systems based on the hydroxo compounds of transition metals and methods for the stabilization of hydroxides. An increasing number of recent publications [26–29] were devoted to confirm the validity of the fundamental conclusion on the hydroxide nature of true catalysts for the oxidation of water.

The hydroxo compounds of Ru, Co, and Mn were immobilized onto the surface of the solid oxide supports TiO_2, NaA, NaX, α-Al_2O_3, and γ-Al_2O_3 for developing effective hydroxide catalysts, which manifest maximum catalytic activity and selectivity in the process of oxygen release in the presence of $Ru(bpy)_3^{3+}$ at pH 6.0 [30]. The activity of all of the Ru-containing catalysts obtained at 373 K was found extremely low (Table 2). However, the samples calcined at 500 K in air or in a vacuum after the immobilization of hydroxides manifested higher activity and selectivity. It is interesting that all of the calcined samples (except for a catalyst on γ-Al_2O_3) were similar to each other in terms of both activity and selectivity regardless of their nature and specific surface area. In all of the tested samples, ruthenium underwent reduction in the course of synthesis by approximately 30% from the initial state Ru(IV) to Ru(III), and a considerable amount of supported ruthenium was converted into the state RuO_4 under the action of $Ru(bpy)_3^{3+}$ in the course of catalytic reaction as a result of oxidative corrosion. However, this deep oxidation of ruthenium was not reflected in its catalytic activity. Upon the storage of ruthenium catalysts in air for a month, the formation of RuO_4 in significant quantities was not detected and the yield of oxygen and catalytic activity remained unchanged.

Supported Co-containing catalysts (Table 3) can be subdivided into two groups. The first group includes the samples supported on TiO_2, NaA, and α-Al_2O_3. Their heat treatment at 500 K noticeably improved catalytic properties; in this case, the samples obtained from ammonium complexes or a hydroxide sol manifested high activity. The second group includes the samples supported onto γ-Al_2O_3 and SnO_2. Their heat treatment at 500 K did not influence catalytic properties, and the samples synthesized from cobalt(III) ammoniate were almost inactive. As in the case of Ru-containing samples, the immobilization of Co(III) compounds on these carriers was accompanied by the reduction of a substantial part of Co(III) ions to Co(II), especially, in the catalysts obtained from the ammoniate. For example, upon the supporting of cobalt onto TiO_2, 60–70% metal was converted into a bivalent form. After storage for one or two months in air, the activity of these catalysts decreased by a factor of 1.5–2. The activity of catalysts from the first group could be restored by calcining them in air at 500 K.

Table 1. Yield of oxygen in the reactions of water oxidation by the $Ru(bpy)_3^{3+}$ complex in the presence of metal phthalocyanines* [21]

Catalyst	pH		Yield of O_2, % (on a stoichiometric basis)
	initial	final	
$CoCl_2$	10	4–5	60
$CoCl_2$	6	3	49
$CoCl_2 : C_4H_6O_6 = 1 : 1$	10	4–5	70
$CoCl_2 : C_4H_6O_6 = 1 : 2$	10	4–5	55
$CoCl_2 : C_6H_8O_7 = 1 : 1$	10	4–5	53
$CoCl_2 : C_6H_8O_7 = 1 : 2$	10	4–5	34
$[Co(bpy)_3](ClO_4)_3$	10	4–5	70
$[Co(bpy)_3](ClO_4)_3$	6	3	62
$[Co(NH_3)_6]Cl_3$	10	4–5	10
$[Co(NH_3)_5Cl]\ Cl_2H_2O$	10	4–5	39
$[Co(NH_3)_5\ H_2O]Cl_3$	10	4–5	42
cis-$[Co(NH_3)_4(H_2O)_2]Cl_3$	10	4–5	65
cis-$[Co(en)_2Cl_2]Cl$	10	4–5	68
cis-$[Co(en)_2Cl_2]Cl$	6	3	48
trans-$[Co(en)_2Cl_2]Cl$	10	4–5	62
$FeCl_3$ (10^{-3} mol/L)	10	4–5	34
$[Fe_2O(phen)_4]Cl_4$ (4×10^{-4} mol/L)	10	4–5	55

* [Metal phthalocyanines] = 10^{-4} mol/L and =$[Ru(bpy)_3^{3+}] = 9 \times 10^{-4}$ mol/L.

Designations: bpy is 2,2'-bipyridine, phen is 1,10-phenanthroline, en is ethylenediamine, $C_4H_6O_6$ is tartaric acid, and $C_6H_8O_7$ is citric acid.

The synthesized Mn catalysts contained bi-, three-, and tetravalent manganese ions. As the Co catalysts, they can also be subdivided into the following two groups: active (NaA, α-Al_2O_3, and γ-Al_2O_3) and low-activity supports (TiO_2, SnO_2, and SiO_2) (Table 4). The distinctive special feature of the Mn catalysts is the presence of ions in two and/or even in three different valence states in their composition regardless of the initial state of manganese in the precursor. The catalytic activity of manganese catalysts synthesized from Mn(III) and Mn(IV) on different supports and dried at 373 K was approximately the same, and it did not increase after heat treatment at 500 K in contrast

Table 2. Yield of oxygen on the 0.3%Ru/support catalysts [30]

Support	Yield of O_2, % (on a stoichiometric basis)	
	calcination temperature, K	
	373	500
TiO_2	27	56
NaA	–	38
NaX	–	40
α-Al_2O_3	8	46
γ-Al_2O_3	–	22

Catalyst sample, 25 mg; $[Ru(bpy)_3^{3+}] = 10^{-3}$ mol/L; pH 6.0; pyrophosphate buffer solution; 298 K.

Table 3. Yield of oxygen on the 0.5% Co/support catalysts [30]

Support	Initial Co solution	Yield of O_2, % (on a stoichiometric basis)	
		calcination temperature, K	
		373	500
TiO_2	Colloidal CoO(OH)	42	55
	$Co(NH_3)_2(H_2O)_4^{3+}$	39	49
NaA	Colloidal CoO(OH)	51	57
	$Co(NH_3)_2(H_2O)_4^{3+}$	47	60
α-Al_2O_3	Colloidal CoO(OH)	21	Not determined
	$Co(NH_3)_2(H_2O)_4^{3+}$	23	56
	$CoCl_2$	0	42
γ-Al_2O_3	Colloidal CoO(OH)	22	22
	$Co(NH_3)_2(H_2O)_4^{3+}$	0	0
	$CoCl_2$	0	12
SnO_2	Colloidal CoO(OH)	42	44
	$Co(NH_3)_2(H_2O)_4^{3+}$	0	0
	$CoCl_2$	0	0

Catalyst sample, 25 mg; $[Ru(bpy)_3^{3+}] = 10^{-3}$ mol/L; pH 6.0; pyrophosphate buffer solution; 298 K.

to the Co-containing samples. In order to establish at which degree of manganese oxidation (III or IV) the greatest activity was reached, a number of catalysts containing the equimolar mixtures of Mn(III)/Mn(II) or Mn(III)/Mn(IV) were synthesized in order to shift the following well-known disproportionation equilibrium to the left at a constant total manganese content:

$$2Mn(III) \rightleftarrows Mn(II) + Mn(IV).$$

With the use of NaA and α-Al_2O_3 supports, this led to an increase in the yield of oxygen. The yield further increased after preliminary heat treatment at 500 K. In the samples on γ-Al_2O_3, an improvement in the catalytic characteristics was not found with the use of any preparation method. The oxidation of a catalyst with concentrated nitric acid considerably decreased its activity. Based on the results obtained, a conclusion was made that the mixture of Mn(III)/Mn(IV) with the predominance of a trivalent form was the most active.

It is well known that the heating of massive hydroxides is accompanied by the release of water: adsorbed water and a large portion of chemically bound or coordinated water are released at 373 and 500 K, respectively. Therefore, it was hypothesized that special surface oxide–hydroxide compounds with specific composition and structure are responsible for the catalytic activity [30]. This also follows from catalyst deactivation as a result of prolonged calcination (for more than 1 h) at 500 K. On the contrary, the reverse adsorption of water from air could be responsible for the deactivation of catalysts in the course of their prolonged storage. The strong influence of the support on the catalytic characteristics of the samples can be explained by the fact that the support is responsible for not only the particle size but also the structure of supported hydroxides. Furthermore, the yield of oxygen in the reaction of water oxidation substantially depends on a buffer solution necessary for maintaining the pH of solution. In the course of reaction (VIII), the addition of a buffer was accompanied by the acidification of solution. Thus, all other factors being equal, the yields of oxygen on 1% Fe-containing catalysts immobilized on α-Al_2O_3, and γ-Al_2O_3 with the use of a phosphate buffer solution differed more than twice (47 and 17% respectively), whereas the yields on both of the catalysts in the presence of a pyrophosphate buffer solution were the same (43%). On all of the test catalysts, the yield of oxygen in an unbuffered medium with the initial value of pH 6–9 was considerably lower. It is believed that the cleavage of bridging oxygen bonds occurs in the particles of hydroxo compounds under the action of buffer anions to cause the disintegration of large hydroxide particles with the formation of smaller fragments. Direct evidence for the validity of this assumption is a multiple increase in the intensity of the EPR spectrum of manganese catalysts after their interactions with an acetate or phosphate buffer solution.

MICROHETEROGENEOUS (COLLOIDAL) HYDROXIDE CATALYSTS

Interest in the colloidal catalysts of water oxidation is caused by the following two basic factors: (1) pros-

Table 4. Yield of oxygen on the 0.5% Ru/support catalysts [30]

Support	Initial state of Mn	State of Mn in reaction	Yield of O_2, % (on a stoichiometric basis)	
			calcination temperature, K	
			373	500
NaA	$MnCl_2$	II	7	–
	$MnCl_2 + H_2O_2$	III	14	–
	$Mn(bpy)(H_2O)Cl_3$	III	25	25
	$Mn(bpy)(H_2O)Cl_3 : MnCl_2 = 1 : 1$	III, II	35	40
	$Mn(bpy)Cl_4$	IV	22	–
	$Mn(bpy)Cl_4 : MnCl_2 = 1 : 1$	IV, II	40	–
α-Al_2O_3	$Mn(bpy)(H_2O)Cl_3$	III	24	30
	$Mn(bpy)(H_2O)Cl_3$, dried in a vacuum	III	21	21
	$Mn(bpy)(H_2O)Cl_3 : MnCl_2 = 1 : 1$	III, II	33	43
	$Mn(bpy)(H_2O)Cl_3 : MnCl_2 = 1 : 1$, dried in a vacuum	III, II	31	33
	$Mn(bpy)(H_2O)Cl_3 : MnCl_2 = 1 : 1$, treated with conc. HNO_3	III, II	–	16
	$Mn(bpy)Cl_4$	IV	18	22
γ-Al_2O_3	$Mn(bpy)(H_2O)Cl_3$	III	26	44
	$Mn(bpy)(H_2O)Cl_3 : MnCl_2 = 1 : 1$	III	34	40
TiO_2	$Mn(bpy)(H_2O)Cl_3$	III	28	19
	$Mn(bpy)(H_2O)Cl_3$, dried in a vacuum	III	24	19
	$Mn(bpy)(H_2O)Cl_3 : MnCl_2$= 1:1	III, II	23	19
	$Mn(bpy)Cl_4$	IV	28	25
	$Mn(bpy)Cl_4$, treated with conc. HNO_3	IV	18	–
	$Mn(bpy)Cl_4 : MnCl_2 = 1 : 1$	IV, II	22	30
SiO_2	$Mn(bpy)(H_2O)Cl_3$	III	14	9
	$Mn(bpy)(H_2O)Cl_3 : MnCl_2 = 1 : 1$	III, II	14	13
SnO_2	$Mn(bpy)(H_2O)Cl_3$	III	29	32

Catalyst sample, 25 mg; $[Ru(bpy)_3^{3+}] = 10^{-3}$ mol/L; pH 6.0; pyrophosphate buffer solution; 298 K.

pects for the development of the molecular systems of artificial photosynthesis based on lipid vesicles in which the reactions of water oxidation and reduction are spatially separated by a vesicle membrane and (2) the possibility of establishing the true mechanism of the catalytic oxidation of water because the colloidal form of a catalyst makes it possible to use jet methods for studying the kinetics of fast reactions with the use of UV–Vis spectroscopy for the identification of the test processes.

Stabilizing compound ligands, which prevent the coagulation of nanosized particles with the formation of a massive hydroxide phase, are necessary for the stabilization of colloidal hydroxide particles in an aqueous medium. The use of compounds to be coordinated to a hydroxide particle through a nitrogen-containing group for this purpose was not promising because these groups are much stronger electron donors than –OH or H_2O, and this leads to the predominant oxidation of the ligands rather than water. Therefore, Elizarova et al. [31] used polyvinyl alcohol (PVA) as a stabilizing agent. The soluble salts of Co(III), Fe(III), Bi(III), Ce(IV), Al(III), and Ti(IV) were hydrolyzed in its presence in the ratio metal : PVA = 2 : 1 (based on the number of hydroxo groups in PVA). Only thus prepared Co and Fe catalysts man-

Table 5. The pH dependences of the initial rate of O_2 formation and the yield of O_2 [31]

Catalyst concentration, mol/L	pH							
	6		6.5		7		7.5	
	$v^0_{O_2}$*	S_{O_2}**	$v^0_{O_2}$*	S_{O_2}**	$v^0_{O_2}$*	S_{O_2}**	$v^0_{O_2}$*	S_{O_2}**
$[Co] = 8.3 \times 10^{-5}$	0.44	22	1.12	43	1.68	50	>2	70
$[Fe] = 8.9 \times 10^{-5}$	O_2 was not released				0.11	29	0.4	42

* $v^0_{O_2}$, mol L^{-1} s^{-1}.

** S_{O_2}, % (on a stoichiometric basis).

ifested activity in the reaction of water oxidation under the action of $Ru(bpy)_3^{3+}$. Their average particle size found by small-angle X-ray diffraction was 2–3 nm. Upon the aging of colloidal catalysts for 48 h, noticeable acidification of solutions was observed and their electronic absorption spectra changed. Furthermore, the particle size noticeably increased. The catalytic properties also changed: the yield of oxygen considerably decreased, but the rate of consumption of the oxidant remained unchanged or even increased. In contrast to heterogeneous catalysts, colloidal Co(III) hydroxide was considerably superior to a colloidal Fe(III)-containing sample in terms of activity and selectivity (Table 5). This was caused by a significant influence of the pH of reaction medium and the acidity of catalytically active M–OH groups coordinated to metal ions.

Elizarova et al. [32] proposed to use water-soluble starch (amylase) as a natural analog of polyvinyl alcohol for the stabilization of manganese(II), (III), and (IV) hydroxides. A study of the influence of synthesis conditions on the catalytic properties of the samples synthesized from a complex of Mn(III) showed that the synthesis temperature is the most important factor, whereas the role of manganese (in a range from 1×10^{-3} to 5×10^{-3} mol/L) and starch (0.01–0.1%) concentrations and pH (samples 9–11, Fig. 3c) is not so significant. In this case, the samples synthesized under identical conditions were noticeably different in catalytic properties. The intensity of the UV–Vis spectra of these samples was also (samples 1–8, Fig. 3a). However, noticeable correlations between the values of $v^0_{O_2}$ and S_{O_2} (Figs. 3b and 3c) on the one hand and the absorption spectra of catalyst solutions on the other hand were not found.

The study of the influence of the degree of oxidation of manganese (II, III, or IV) on the characteristics of catalysts showed that the samples containing only Mn(II) prepared from $MnCl_2$ were inactive in the process of oxygen evolution; however, they were prone to form massive $Mn(OH)_2$ in an alkaline medium. The catalysts prepared from $Mn(bpy)(H_2O)Cl_3$ containing Mn(III) and those synthesized from the complex $Mn(bpy)Cl_4$, where Mn(IV) is present, were found most active. However, it was established by the titration of them that the solution contained no more than 20% Mn(IV); that is, manganese was reduced to a trivalent state in the course of catalyst synthesis. Upon storage in air, the characteristics of the most active catalysts considerably deteriorated, and this was accompanied by an increase in their Mn(IV) content. The yield of oxygen in the presence of the catalysts synthesized from a mixture of $MnCl_2$ and $KMnO_4$ and containing only Mn(IV) was extremely low (S_{O_2} < 20%). Their reduction by the addition of $MnCl_2$ or hydrazine considerably increased the yield of O_2 (from 15 to 29%). The heating of these samples at 363 K made it possible to increase the yield of oxygen to 40%.

The samples with Mn(III) and Mn(IV), containing PVA were specially prepared for comparing the advantages and disadvantages of the stabilization of catalysts by starch and polyvinyl alcohol. The yield of oxygen in the presence of the Mn(III) sample with a PVA additive was considerably lower (S_{O_2} < 30%) than that in the presence of the catalyst stabilized by starch. The Mn(IV) catalysts stabilized by both starch and PVA were found similar in terms of activity and selectivity. The small-angle scattering study of the samples made it possible to reveal a significant difference in the particle sizes. The freshly prepared starch-containing catalyst predominantly contained small particles of size ~3 nm and a small number of particles of size ~9 nm. On its storage in an atmosphere of argon during seven days, the particles considerably coarsened (their average size reached 11 nm). However, the sample stabilized by PVA mainly consisted of particles with a size of 18 nm.

The results obtained by Elizarova et al. [32] made it possible to make the conclusion that, in contrast to polyvinyl alcohol, starch not only stabilizes colloidal hydroxide particles but also chemically interacts with them through hydroxyl groups thus influencing the process of hydrolysis and the composition of the resulting hydroxo compounds. Hydroxides stabilized by starch are comparable with the hydroxides on oxide supports in their catalytic properties (the yield of oxy-

gen at pH 7–9 is 65–75%). Surprisingly, it was found that, upon the stabilization of hydroxide nanoparticles by readily oxidizable macromolecules, these latter are almost not oxidized.

Thus, the above results unambiguously indicate that an effective catalyst for the oxidation of water should contain Mn(III) and Mn(IV) with the predominance of a trivalent form in the initial state. This conclusion is consistent with the recent data on the electronic state of the oxygen-releasing complex of photosystem II, which, most probably, contains three Mn(III) atoms and one Mn(IV) atom in the state S_0 [7, 33].

Elizarova et al. [34] stabilized the colloidal hydroxides of Co(III) by starch (0.01–0.5 wt %). The catalytic activity substantially depended on the quantity of added starch, the temperature of synthesis, and the nature of a buffer solution in which the oxidation of water was conducted. The catalyst containing 0.01% starch remained transparent for several weeks; however, the yield of oxygen in its presence decreased from 65 (in the absence of starch) to 55%. As the starch content was increased to 0.5 wt %, the yield of oxygen in reaction (VIII) sharply decreased. However, the preliminary heat working of starch in air at 430 K for 8 h, which leads to its destruction to molecules with smaller molecular weights, made it possible to avoid a decrease in selectivity for the formation of oxygen even at this high stabilizer content. The catalysts with the high concentration of the thermally activated starch (0.5 wt %) retained their properties even upon storage for a month. A study of the optical absorption spectra of the Co-containing samples prepared with different starch concentrations showed that, in the solutions containing this stabilizer in larger amounts, the catalysts were the hydroxo compounds of Co(III), which were formed at the initial stages of hydrolysis and contained many bridging μ-OH groups binding cobalt ions. At the same time, in the solutions with a low concentration of starch (0.01%), the oxolation of primary hydroxide particles and the formation of μ-O bridging bonds between the ions of Co occurred. With an increase in the catalyst synthesis temperature, the oxolation was accompanied by a shift of the optical absorption band of the catalyst to a long-wave region, which was explained by the replacement of coordinated OH groups by oxo ligands because of the deepening of hydrolysis. The important consequence of the processes taking place is a decrease in the solubility of hydroxides in the buffer media. An increase in the concentration of starch and in the size of its molecules or associates worsens the catalytic properties of colloidal hydroxides.

Elizarova et al. [35] stabilized the colloidal hydroxide of Fe(III) with starch and studied the influence of a buffer medium on the spectra of Fe-containing catalysts stabilized by 0.5% starch. The optical absorption spectrum of the freshly prepared colloidal solution of iron hydroxide (in the absence of starch), which was

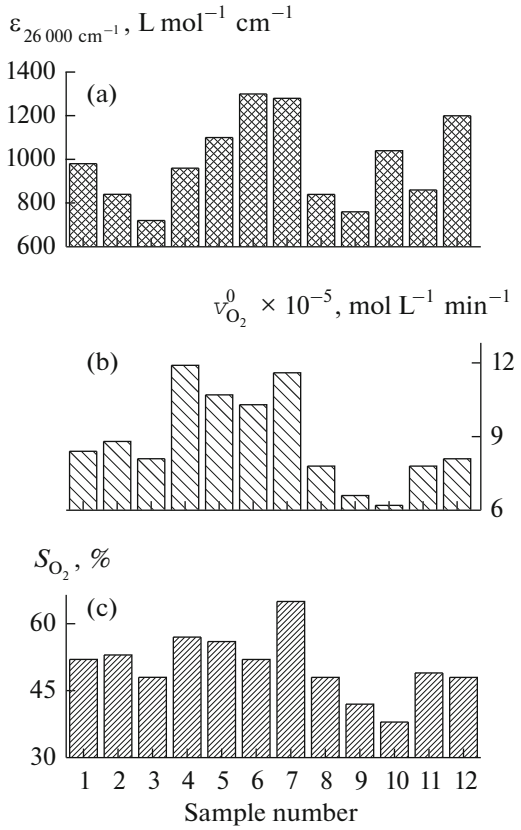

Fig. 3. Catalytic properties of Mn samples (nos. 1–12) containing 0.1% starch synthesized from $Mn(bpy)Cl_3(H_2O)$ [32]: (a) the UV–Vis spectra of the samples, (b) the initial rate of O_2 formation, and (c) the yield of O_2. Reaction conditions: [Mn] = 10^{-4} mol/L; $[Ru(bpy)_3^{3+}] = 10^{-3}$ mol/L; 0.1 M phosphate buffer solution with pH 7; 298 K. The concentrations of Mn in the initial catalyst solutions: (nos. 1–10) 2.5×10^{-3}, (no. 11) 10^{-3}, and (no. 12) 5×10^{-3} mol/L. The synthesis temperature of sample nos. 9 and 10 was 298 K, and that of the other samples was 363 K.

prepared by the heating of a solution of iron nitrate at pH 2, was similar to the spectrum of the catalyst containing starch, but it was different from it in intensity. The yields of oxygen in the presence of these catalysts at pH 9 were close to each other (53% in the presence of starch and 62% in its absence), but they were essentially different at pH 7.5 (48 and 25%, respectively). Thus, it was found that the intensity of the absorption spectrum of a Fe-containing catalyst does not correlate with its activity.

In order to determine what form of a hydroxo compound is active in the reaction of water oxidation, the properties of hydroxo polymers and low-molecular-weight hydroxo complexes with accurately determined structures were studied with the use of Fe(III) as an example [35]. The compounds in which the distance between adjacent iron atoms was minimal and which

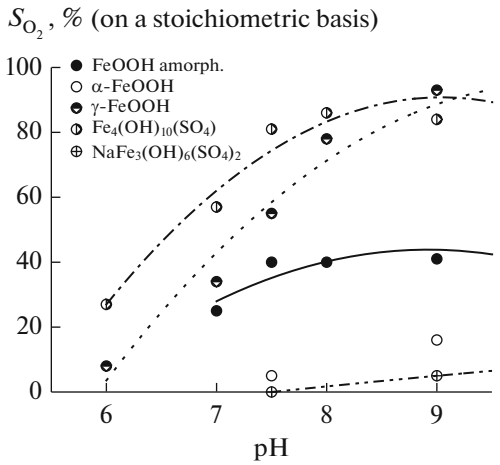

Fig. 4. Dependence of the yield of oxygen on the pH of reaction medium in the presence of heterogeneous Fe(III) hydroxide catalysts [35]. Reaction conditions: pyrophosphate buffer solution (0.05 mol/L); catalyst weight, 20–50 mg; $[Ru(bpy)_3^{3+}] = 10^{-3}$ mol/L; 298 K.

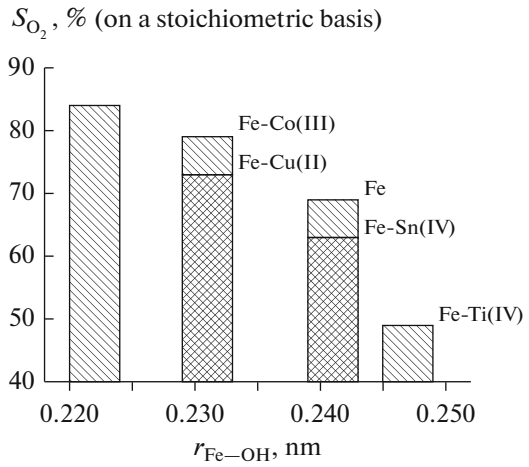

Fig. 5. Dependence of the yield of oxygen on the Fe–OH bond length in binary hydroxides [36]. Catalyst weight, 20 mg; $[Ru(bpy)_3^{3+}] = 2 \times 10^{-3}$ mol/L; pH 9; 298 K.

were saturated with acidic terminal hydroxyl groups were found most selective and active (Fig. 4). The maximum yields of oxygen were observed in the presence of γ-FeOOH ($S_{O_2} = 93\%$) and $Fe_4(OH)_{10}(SO_4)$ ($S_{O_2} = 87\%$). The structural characteristics of $Fe_4(OH)_{10}(SO_4)$ and $NaFe_3(OH)_6(SO_4)_2$, in the presence of which maximum and minimum yields of oxygen, respectively, were measured, were studied by an EXAFS method and IR spectroscopy. The main differences in the structures of these compounds were manifested in the coordination of sulfate anions and in distances between the adjacent atoms of iron (3.0 Å in $Fe_4(OH)_{10}(SO_4)$, where the atoms were coordinated to each other through faces, and 3.6 Å in $NaFe_3(OH)_6(SO_4)_2$, where coordination through apexes occurred). The fact that the compounds $NaFe_3(OH)_6(SO_4)_2$ and α-FeOOH are maximally different in the total numbers of surface hydroxyl groups (4.7 and 0.1 mmol/g, respectively) but they ensure the equally low yields of oxygen under identical conditions (at pH 9.5, $S_{O_2} = 16\%$) makes it possible to draw the conclusion that not all of the hydroxyl groups but only those coordinated to the ions of Fe(III) and meet three conditions are responsible for the catalytic properties. First, the active hydroxo groups should be close to each other (as, for example, in $Fe_4(OH)_{10}(SO_4)$ and $NaFe_3(OH)_6(SO_4)_2$). Second, the oxidation of terminal hydroxo groups is energetically more favorable from the thermodynamical point of view: the samples containing their greatest amounts (γ-FeOOH and $Fe_4(OH)_{10}(SO_4)$) were maximally effective. Third, these hydroxyl groups should possess high acidity; the acidity of hydroxo groups in γ-FeOOH and $Fe_4(OH)_{10}(SO_4)$ is maximal because of their special structure, namely, the presence of a large number of hydrogen bonds, which contribute to the formation of strong acid sites.

The influence of the acidity of terminal hydroxo groups on the catalytic activity was investigated based on the example of binary Fe(III) hydroxides also containing the ions of Ce(IV), Co(III), Cu(II), Sn(IV), and Ti(IV) [36] (Fig. 5). The presence of foreign ions causes a redistribution of electron density on the ions of Fe and, correspondingly, a change in the Fe–OH bond length. The yield of oxygen in the presence of the above catalysts is directly correlated with the Fe–OH distance. It is very probable that a decrease of the length of this bond strengthens the acidic properties of the OH group coordinated to the active center and thus improves the catalyst properties in the reaction of water oxidation. Therefore, the acidity of the hydroxyl groups of a catalyst is a key factor affecting its activity in the process of water oxidation.

The studies of nanosized hydroxo compounds as water oxidation catalysts were resumed at the Boreskov Institute of Catalysis, Siberian Branch of the Russian Academy of Sciences in 2015. The study of the hydroxo compounds of Fe, Mn, Co, and Cu stabilized by starch with the use of transmission electron microscopy photon-correlation spectroscopy made it possible to refine the structure of the catalysts and the special features of their aging. New data on the kinetics of the catalytic oxidation of water in the presence of hydroxide catalysts [37], which were obtained by a stopped flow method with the use of UV–Vis spectroscopic detection, are indicative of the extremely high specific activity of these catalysts: at a borate buffer concentration of 0.06 mol/L, pH 10, a temperature of 298 K, $[Ru(bpy)_3^{3+}] = 5 \times 10^{-4}$ mol/L, [Fe] = 10^{-6} mol/L, and [Co] = 5×10^{-5} mol/L, the turnover frequency of the

catalyst was $TOF_{Fe} \approx 220\ s^{-1}$ or $TOF_{Co} \approx 40\ s^{-1}$ (specific activity or the value of TOF characterizes a maximum number of moles of the product formed per unit time at an active site of the catalyst). The obtained values of TOF are in order of magnitude close to the activity of the natural oxygen-releasing complex of photosystem II, where TOF varies from 100 to 400 s^{-1} [16].

MECHANISM OF THE OXIDATION OF WATER IN THE PRESENCE OF HYDROXIDE CATALYSTS

The development of new catalysts for a chemical process requires a sufficiently clear knowledge of the mechanism of their action, which makes it possible to change from a combinatory (empirical) approach to the target-oriented scientifically grounded design.

The kinetics of oxygen evolution in a reaction with the participation of a trisbipyridyl complex of ruthenium the presence of hydroxide catalysts immobilized on the oxide supports of TiO_2 and Al_2O_3 was studied in order to determine the mechanism of water oxidation by reaction (VIII) [38]. It was found that the yield of oxygen passed through a maximum depending on pH, catalyst amount, and oxidant concentration. The reactant concentration ranges in which the maximum yields of oxygen were reached depended on the nature of a support, the amount of supported hydroxide, the pH of a medium, and nature of a buffer solution (Fig. 6b). The reduced form of the trisbipyridyl complex of ruthenium $Ru(bpy)_3^{2+}$ exhibited an inhibiting effect, which manifested itself in a decrease in the yield of oxygen upon the complete consumption of an oxidizing agent. The inhibiting effect was also found upon the addition of the reduced form of the oxidizing agent into the reaction solution before the introduction of $Ru(bpy)_3^{3+}$ into the solution. The preliminary addition of anions, for example, ClO_4^-, which form a sparingly soluble salt with this complex, considerably decreased the rate of reaction but increased the yield of oxygen by a factor of 1.5–2, and the apparent order of reaction with respect to oxidant concentration changed in this case from first to zero (Fig. 6a). It was noted that the activity of a Co catalyst and the yield of oxygen on it in the absence of $NaClO_4$ were much higher than those on a Mn-containing sample were. The yields of O_2 in the Co- and Mn-containing systems without ClO_4^- were 8×10^{-5} and 4×10^{-5} mol/L, respectively, whereas they became approximately equal (12×10^{-5} mol/L) in the presence of ClO_4^-.

The addition of colloidal catalysts stabilized with PVA and other complexes bearing a positive charge, for example, $Co(bpy)_3^{3+}$ or $Co(NH_3)_5Cl^{2+}$, also led to a decrease in the rate and selectivity of the formation of oxygen (Table 6). This effect is a direct consequence

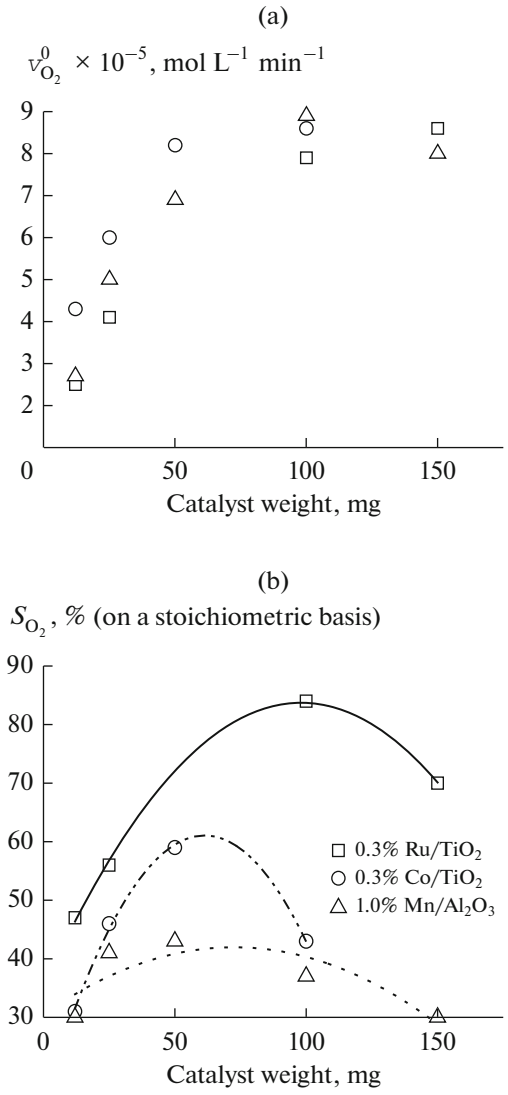

Fig. 6. Dependences of (a) the initial rate of oxygen formation and (b) the yield of oxygen on catalyst weight [38]. Pyrophosphate buffer solution with pH 6.0 at 298 K.

of competitive adsorption between the reduced and oxidized forms of a ruthenium complex on the active sites of the catalyst. In order to simplify a study of the mechanism of water oxidation, stabilized colloidal catalysts based on the hydroxo compounds of transition metals were prepared [31]. The use of colloidal samples makes it possible to study the kinetics of not only oxygen evolution but also the consumption of an oxidant and/or the appearance of its reduced form by UV–Vis spectroscopy. The hydroxides of Co(III) and Fe(III) were stabilized by PVA in a weight ratio of 2 : 1. These samples possessed all of the properties characteristic of supported hydroxide catalysts, including the bell-shaped dependences of the yield of oxygen on pH and on the concentrations of a catalyst and an oxidizing agent and also the manifestation of the inhibiting action of the reduced form of the oxidizing agent.

Table 6. Effect of the additives of cationic complexes on the initial rates of O_2 formation and $Ru(bpy)_3^{3+}$ consumption and on the yield of O_2 [31]

Additive, mol/L	Catalyst								
	[Co] = 2×10^{-5} mol/L, pH 7			[Co] = 8.3×10^{-5} mol/L, pH 7			[Fe] = 8.9×10^{-5} mol/L, pH 7.5		
	$v_{O_2}^0$*	v_{Ru}^0**	S_{O_2}***	$v_{O_2}^0$*	v_{Ru}^0**	S_{O_2}***	$v_{O_2}^0$*	v_{Ru}^0**	S_{O_2}***
With no additive	1.44	10.4	56	1.68	13.4	50	0.40	3.8	42
$[Ru(bpy)_3^{2+}] \times 10^3$	0.56	5.8	39	0.94	9.8	39	0.03	3.1	4
$[Co(bpy)_3^{2+}] \times 10^3$	0.56	10.4	22	1.12	14.6	31	0.06	3.6	7

* $v_{O_2}^0 \times 10^4$, mol L^{-1} min^{-1}.

** $v_{Ru}^0 \times 10^4$, mol L^{-1} min^{-1}.

*** S_{O_2}, % (on a stoichiometric basis).

However, in contrast to the supported catalysts, colloidal Co(III) hydroxides were found much more active than Fe(III) hydroxides (Table 6).

The observed pH dependence of catalytic activity can be caused by the ion-exchange nature of the first stage of water oxidation:

$$M^{III}\text{–}OH \rightleftarrows M^{III}\text{–}O + H^+, \quad \text{(IX)}$$

$$M^{III}\text{–}O^- + Ru(bpy)_3^{3+} \rightarrow M^{III}\text{–}O^-\cdots Ru(bpy)_{3,ads}^{3+}. \quad \text{(X)}$$

Here, M^{III} is the catalytically active center of Co(III) or Fe(III) hydroxide. Note that the hydroxo group M^{III}–OH should possess special acid–base properties, which provide the possibility of cation exchange in a narrow range of pH. Elizarova et al. [31] hypothesized that a deprotonated hydroxo group coordinated to a strong oxidizing agent is formed in reaction (X). Finally, this leads to electron transfer and the formation of an active oxygen species, probably, chemisorbed at the active center of the catalyst:

$$M^{III}\text{–}O^-\cdots Ru(bpy)_{3,ads}^{3+} \rightarrow M^{II}\cdots O_{ads}^*\cdots Ru(bpy)_{3,ads}^{2+} \quad \text{(XI)}$$

$$\text{or } M^{III}\text{–}O^-\cdots Ru(bpy)_{3,ads}^{3+} \rightarrow M^{IV}\text{–}O^{-\bullet}\cdots Ru(bpy)_{3,ads}^{2+} \rightarrow M^{II}\cdots Ru(bpy)_{3,ads}^{2+} \quad \text{(XIa)}$$

Of course, the catalytically active fragments M^{III}–OH should be located sufficiently close to each other in order to form molecular oxygen from two chemisorbed oxygen atoms according to the reaction

$$2[M^{II}\cdots O_{ads}^*\cdots Ru(bpy)_{3,ads}^{2+}] + H_2O \rightarrow 2M^{II}(H_2O) + O_2 + 2Ru(bpy)_3^{3+}. \quad \text{(XII)}$$

The following side reaction, which does not lead to the release of molecular oxygen, with the destruction of organic ligands, for example, bipyridine, was also considered:

$$M^{III}\text{–}O^-\cdots Ru(bpy)_{3,ads}^{3+} \rightarrow M^{II}(H_2O) + Ru(bpy)_2(bpy\text{-}ox)^{2+}, \quad \text{(XIIa)}$$

where bpy-ox is the product of the partial oxidation of a bipyridyl ligand. It is believed that the reduction of a catalytically active center by the following oxidant molecule is the final stage of the process:

$$M^{II}(H_2O) + Ru(bpy)_3^{3+} \rightarrow M^{III}\text{–}OH + H^+ + Ru(bpy)_3^{2+}. \quad \text{(XIII)}$$

According to Elizarova et al. [31], the rate of the overall process is determined by the rate of stage (XII) of the primary oxidation of the active center. In the case of the Ru-containing catalysts, changes in the oxidized state of a catalytically active ion is described by the transitions M(IV)–OH → M(IV)–$O^{-\bullet}$ → M(III)–OH → M(IV)–OH.

The results of a simulation based on the proposed kinetic scheme of reaction (VIII) are consistent with the experimental kinetic data obtained on a Co(III)/TiO_2 catalyst. This is concerned with the following process characteristics: (1) reaction inhibition accompanied by a decrease in the yield of oxygen upon the addition of $Ru(bpy)_3^{2+}$ to the reaction, (2) zero-order overall reaction in the absence of the inhibiting action of $Ru(bpy)_3^{2+}$, and (3) the bell-shaped dependence of the yield of oxygen on the initial reactant and catalyst concentrations and pH. The results of the simulation on a qualitative level reflect these special features; however, a precise quantitative correlation between experimental and calculated data was not achieved, and this fact was explained [30] by the use of a somewhat tentative model.

The next stage of the study of the mechanism of reaction (VIII) was a stopped-flow investigation of its kinetics in the presence of colloidal Co(III) hydroxide stabilized by starch [39]. A study of the consumption of an oxidizing agent (an absorption maximum at a wavelength of 675 nm) and the buildup of the concentration of its reduced form (an absorption maximum at 452 the nm) at the initial $Ru(bpy)_3^{3+}$ concentration = 5×10^{-5} mol/L and a temperature of 298 K in 0.03 M borate buffer solution with pH 9.18 showed that, after the rapid consumption of 80–90% oxidizing agent (in 0.03 s), the decrease in the optical absorption at a wavelength of 675 nm sharply slowed down and then the absorption slowly disappeared (with a duration to 0.3 s). Moreover, at [Co] > 2.5×10^{-4} mol/L (when the appearance of a reduced form of the oxidizing agent cannot be detected as a result of a short characteristic reaction time in comparison with the time resolution of the utilized installation), only the disappearance of this absorption at 675 nm was observed with a first-order rate constant of ~2 s^{-1}. It was assumed that the above absorption was due to an intermediate of reaction (VIII). The absorption spectrum of the intermediate, which was restored point-by-point in a range from 460 to 680 nm, exhibited a maximum at 568 nm. Note that Khannanov et al. [40], who studied reaction (VIII) in the presence of cobalt salts, also detected an intermediate; however, its absorption was in the region of 800 nm. Therefore, Pestunova et al. [39] made a conclusion on the existence of an intermediate product of oxidant degradation. The absorption intensity of this intermediate was directly proportional to the concentrations of both a catalyst and an oxidant, and this fact indicates that the observed intermediate was the product of a reaction of the catalyst with the oxidant. This can be either a product of the partial oxidation of water coordinated to the active center of the catalyst, that is, a peroxo complex of cobalt, or a product of the side reaction of the catalytic degradation of the oxidant, that is, a complex of ruthenium with partially oxidized ligands. It is significant that the absorption spectrum of the intermediate was wide, and this is more characteristic of colloids than of the individual complexes of metals. Furthermore, the majority of ruthenium(II) complexes with bipyridyl and similar ligands are very stable, and they cannot disappear at the experimentally observed high rate in the absence of an oxidizing agent. The complexes of ruthenium(II) with the bipyridyl ligands absorb in the region of shorter wavelengths, and they are characterized by extinction coefficients $\varepsilon > 10000$ L mol^{-1} cm^{-1}, whereas the extinction coefficient of the intermediate was estimated at several hundred units. This fact made it possible to assume that the optically detected intermediate was a peroxo complex of colloidal cobalt hydroxide. The conclusion drawn was confirmed by the results of recent publications dedicated to studies of the electrochemical oxidation of water on the electrodes covered with α-Fe_2O_3, where the formation of peroxide intermediates with an optical absorption maximum at 580 nm and $\varepsilon = 800–1200$ L mol^{-1} cm^{-1} was detected [41–43].

For the quantitative description of the kinetics of reaction (VIII), a kinetic scheme was proposed [39] based on a published formal scheme [31] with the addition of a stage of the ion-exchange adsorption of the reduced form of the oxidant:

$$M^{III}–O^- + Ru(bpy)_3^{2+} \rightarrow M^{III}–O^-\cdots Ru(bpy)_{3,ads}^{2+}. \quad (Xa)$$

Furthermore, stages (XI) and (XIa) were replaced by

$$[M^{III}–O]^+ \cdots Ru(bpy)_3^{3+} \rightarrow [M^{IV}=O]^{2+} + Ru(bpy)_3^{2+}, \quad (XII^*)$$

$$[M^{IV}–O]^{2+} + Ru(bpy)_3^{3+} \rightarrow M^{III}OH + Ru(bpy)_2(bpy\text{-}ox)^{2+}. \quad (XIIa^*)$$

If stages (X) and (Xa) are considered quasi-equilibrium and stage (XII*) is a rate-determining stage of the entire process, it is simple to obtain the following expression for the effective first-order rate constant of overall reaction (VIII) on condition that the concentration of $(Co^{IV}O)^{2+}$ and Co^{II} particles:

$$\frac{1}{k_{eff}} \approx \frac{1}{2k_{XII^*}[Co]_\Sigma} \times \left(\frac{1}{K'_X} + \left[Ru(bpy)_3^{3+} + \frac{K'_{Xa}}{K'_X}[Ru(bpy)_3^{2+} \right] \right), \quad (1)$$

where K_X and K_{Xa} are the equilibrium constants of adsorption stages (X) and (Xa), respectively, and k_{XII^*} is the rate constant of stage (XII*).

Expression (1) adequately describes the observed dependences of the effective rate constant of the catalytic reaction on the concentrations of the catalyst, the oxidant, and its reduced form. It was used for evaluating the equilibrium constants K'_X and K'_{Xa} and the constant k_{XII^*}, which determines the rate of the overall process (Table 7).

The detailed reaction scheme proposed for the oxidation of water on cobalt hydroxide [39] includes two conjugated catalytic processes: the oxidation of water (stages (XIV)–(XIX)), the catalytic degradation of bipyridyl (stages (XIV)–(XVIII) and (XXI)–(XXII))), and the spontaneous reaction of bipyridyl degradation (stage (XXIII)).

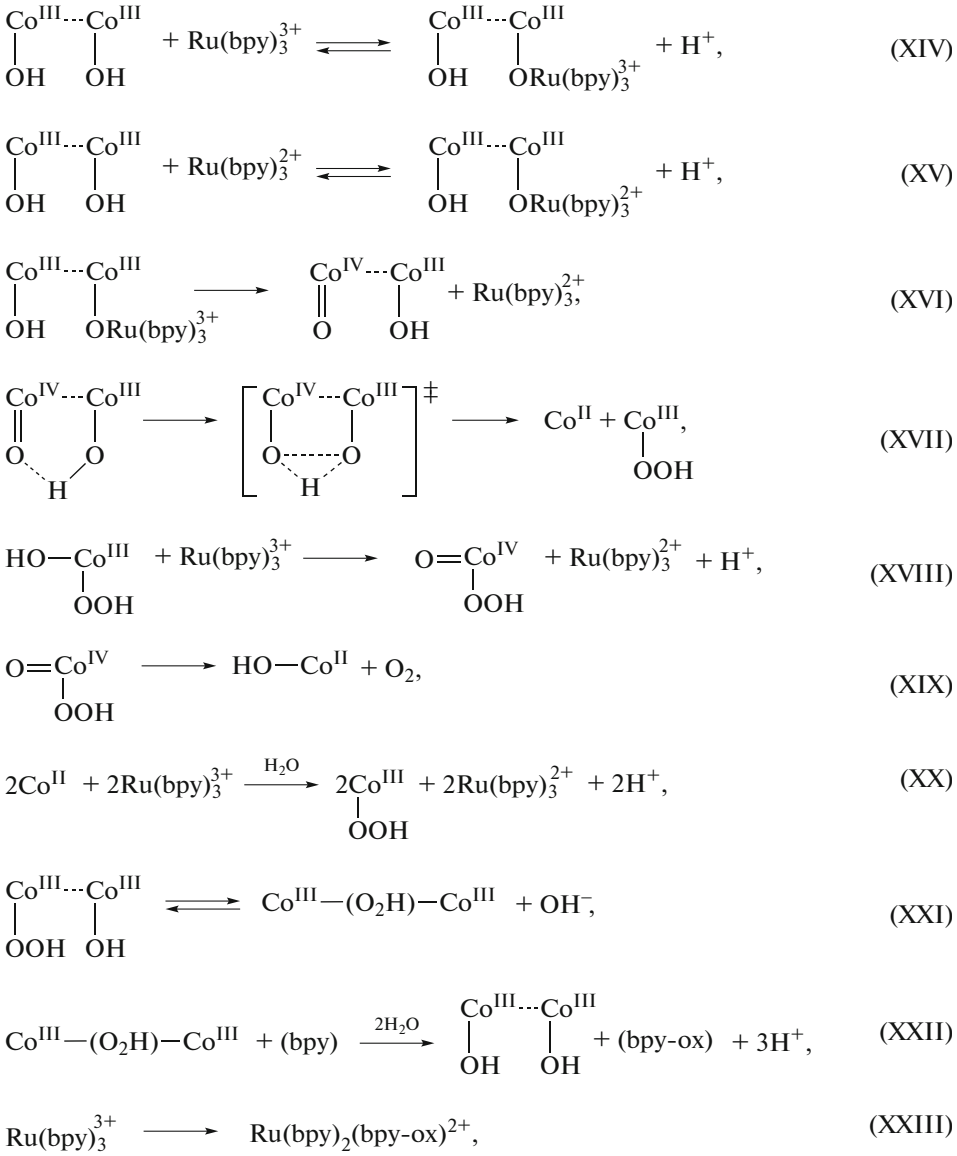

(XIV)

(XV)

(XVI)

(XVII)

(XVIII)

(XIX)

(XX)

(XXI)

(XXII)

(XXIII)

bpy-ox is partially oxidized bipyridyl.

Scheme 1. Hypothetical mechanism of water oxidation by the trisbipyridyl complex of ruthenium in the presence of colloidal of cobalt(III) hydroxide as a catalyst [39].

Published data on the oxidation–reduction and spectral properties of the peroxo complexes of cobalt and a number of other transition metals made it possible to hypothesize that a terminal peroxo group coordinated to the active center of the catalyst is an intermediate in the reaction of water oxidation, and the detected intermediate is a bridging peroxo group, which participates in a side reaction of the catalytic degradation of bipyridyl ligands. A ratio between the rates of these two processes and, consequently, a ratio between the yields of products in both of the channels depend on a ratio between the concentrations of peroxide intermediates, which is determined by reaction conditions. An increase in pH will facilitate not only the occurrence of reaction (XIX) but also a shift of pre-equilibrium (XIV) to the right and, thus, an increase in the yield of oxygen, which was observed experimentally. On the contrary, an increase in the catalyst concentration to the values comparable with the oxidant concentration decreases the yield of oxygen. This can be easily explained by the fact that the probability of the secondary interaction of the oxidant with the same active center (XIX) decreases with increasing catalyst concentration; therefore, a larger number of terminal peroxo complexes active in the reaction of water oxidation manages to pass to a bridging position, which is active in the side reaction.

Table 7. Calculated values of some constants of kinetic equation (1) for reaction (VIII) [39]

Series of experiments	Reactant concentrations, mol/L			k_{XII^*}, s^{-1}	K'_X, L/mol	K'_{Xa}, L/mol
	$[Co]_\Sigma$	$[Ru(bpy)_3^{3+}]^0$	$[Ru(bpy)_3^{2+}]^0$			
1	5×10^{-6}	(5×10^{-5})–(5×10^{-4})	0	1340	2.2×10^5	–
	2.5×10^{-5}	10^{-5}–10^{-3}	0	1380	1.3×10^5	–
	5×10^{-6}	2.5×10^{-4}	(5×10^{-5})–(5×10^{-4})	–	1.2×10^4	$0.92K'_X$
Average values				1360	1.2×10^5	$0.92K'_X$
2	5×10^{-6}	10^{-5}–(5×10^{-4})	0	142	3.2×10^4	–
	2.5×10^{-5}	10^{-5}–(5×10^{-4})	0	146	1.3×10^4	–
	2.5×10^{-6}	2.5×10^{-6}	(5×10^{-5})–(5×10^{-4})	–	6.4×10^3	$0.62K'_X$
	5×10^{-6}	5×10^{-6}	(5×10^{-5})–(5×10^{-4})	–	1.4×10^4	$0.67K'_X$
Average values				143	3.0×10^4	$0.65K'_X$

Reaction conditions: a 0.03 M borate buffer solution; pH 9.2; temperature, 298 K.

SYNTHETIC SYSTEMS, WHICH IMITATE THE ACTION OF NATURAL PHOTOSYSTEM II, BASED ON ZINC PORPHYRINS IMMOBILIZED ON A LIPID VESICLE MEMBRANE

In parallel with a search for effective catalysts of water oxidation, studies oriented to the development of photosensitized systems, which could be an alternative of the trisbipyridyl ruthenium complex and similar compounds, were carried out. Based on the results published by Cristensen et al. [44], Gerasimov et al. [45] attempted to reconstruct a sacrificial system with respect to a primary electron acceptor, in which zinc(II) *meso*-tetrakis(*para*-sulfonatophenyl)porphyrin served as the photocatalyst of water oxidation and the persulfate anion $S_2O_8^{2-}$ served as the primary electron acceptor. The product of the one-electron oxidation of this metal porphyrin, which was generated under the action of visible light in the presence a sacrificial oxidant, manifested high stability. The one-electron oxidation potential of this product measured by cyclic voltammetry was +0.84 V relative to NHE; generally speaking, this makes it possible to hope for the oxidation of water at pH > 7. However, it was impossible to detect oxygen evolution in the presence of colloidal RuO_2 as a catalyst in either light-induced (photocatalytic) or dark (chemical) processes. At the same time, the use of an osmium(III) trisbipyridyl photocatalyst with a close oxidation potential under analogous conditions (in the dark mode) and with the same concentrations made it possible to release ~5% oxygen from water (on a stoichiometric basis). The results of Gerasimov et al. [45] indicate the ineffectiveness of metal porphyrins as photocatalysts because, first, they manifest considerably higher specificity with respect to the catalyst in comparison with traditional oxidants, and, second, the products of the intermediate oxidation of porphyrins are capable of sensitizing the undesirable process of oxygen absorption. Attempting to overcome the above difficulties, Gerasimov et al. [45] considered another porphyrin, zinc(II) *meso*-tetrakis-(*N*-methyl-4-pyridyl)porphyrin (ZnTMPP), and used iron(II) trisbipyridyl as an intermediate electron donor. Thus, the following electron-transfer reaction scheme was implemented:

$$H_2O \rightarrow Co(III) \rightarrow [Fe(bpy)]_3^{2+} \rightarrow ZnTMPP^{4+} \xrightarrow{h\nu} {}^3ZnTMPP^{4+} \rightarrow S_2O_8^{2-}. \quad \text{(XXV)}$$

It was also impossible to detect oxygen evolution in this system at pH 9.2 in the presence of dissolved $CoCl_2$ as a catalyst; this fact can be explained by the absorption of oxygen in the course of the photooxidation of porphyrin. This obstacle could be overcome by the spatial separation of water oxidation and charge separation processes. For this purpose, a colloidal catalyst based on Co(III) hydroxide immobilized on the external membrane of lipid vesicles, in the internal space of which a photocatalyst was contained and an electron transfer system functioned, was used [46]. In this system, a significant yield of oxygen was achieved, and the turnover number (TON) of the photocatalyst based on Co(III) hydroxide was noticeably higher than 1.

QUANTUM-CHEMICAL STUDY OF THE STRUCTURE OF THE OXYGEN-RELEASING CENTER OF A CATALYST AND THE MECHANISM OF WATER OXIDATION

Experimental studies of the test reaction in the presence of hydroxide catalysts performed at the Boreskov Institute of Catalysis, Siberian Branch of the Russian Academy of Sciences were accompanied by studying its probable mechanism using quantum-chemical methods. The simulation of water oxidation on Fe(III) hydroxides was carried out within the

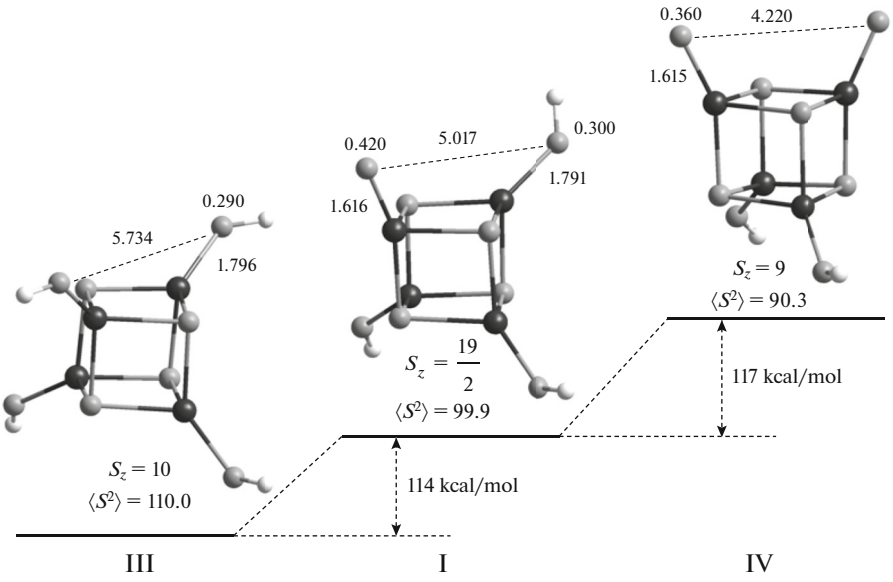

Fig. 7. Initial complex S_0 (III) and its possible states S_1 (I) and S_2 (IV). Henceforth, numerals with three decimal digits refer to bond lengths (in Å), numerals with two decimal digits refer to Mulliken spin densities (in au), and numerals with one decimal digit and integers designate the relative energies of optimized structures (in kcal/mol). For each structure, the spin projection S_z and the expected value of the squared spin $\langle S^2 \rangle$ are given. The atoms of Fe, O, and H are shown in black, gray, and white colors, respectively.

framework of the density functional theory (DFT) in a cluster approximation without explicitly considering the process of electron and proton detachment by an external oxidant, as usually performed in the quantum-chemical calculations of the oxygen-releasing systems (for example, see [47]). The energies of different intermediate structures were compared for the same S_i state of the cycle [48]. Filatov et al. [49] used a model of the four-nuclear iron(III) hydroxide cluster $Fe_4O_4(OH)_4$ (structure III, Fig. 7) with the cubic nucleus Fe_4O_4. This model was chosen for following reasons: Elizarova et al. [20] found that the presence of μ-oxo bridging bonds in hydroxides directly facilitates the formation of oxygen. The γ-FeOOH hydroxides and the synthetic tetrameric complex $Fe_4(OH)_{10}SO_4 \cdot nH_2O$ [35], which are the most selective catalysts for the oxidation of water, contain $Fe(OOH)_6$ octahedrons with common edges. In this case, every three metal cations are located in the apexes of a tetrahedron. Thus, they differed from a cube only in terms of the absence of the fourth center, which was added for simplicity into the model structure in order to stabilize the geometry of the entire system. Because the number of Fe cations directly bound to associated oxygen centers in the process of water oxidation by hydroxide can vary from one to three and not more, a simple cubic model is a reasonable compromise. An important additional advantage of this model is the similarity of the tetrahedral combination Fe_3O_3 with the analogous structural element Mn_3O_3 of the natural oxygen-releasing center Mn_4CaO_5. An analogous model was also used in published studies [47, 50, 51], in which the oxygen-releasing system was simulated based on cobalt hydroxide. The tetramers and dimers considered below in the ground state are ferromagnetic.

In the DFT calculations, the local minimums and transient states in three competing reaction paths of the association of oxo and hydroxo centers were found. All of the reaction paths begin with the detachment of one or two electron + proton pairs by the oxidant (in the calculation, this was achieved by the simple removal of a hydrogen atom and the formation of one or two ferryl groups Fe(IV)=O (structures I and IV, Fig. 7)).

Association of the Oxygen Atom and the Hydroxyl Group at One Center

This route corresponds to the direct binding of terminal oxygen and the hydroxyl group at one Fe center and consists of two stages. Based on hydroxide structure I, the initial hydroxylation of the ferryl group of structure I by the molecule of water is initially required (Fig. 8) with the subsequent detachment of an electron/proton pair from the hydroxyl group and the formation of hydroperoxide XIV (Fig. 9). Thus, the association of the oxygen-containing centers in this route corresponds to transfer into the state S_2.

The transition state at the stage of hydroxylation corresponds to the formation of a hydrogen bond between coordinated water and ferryl oxygen (structure X, Fig. 8). This process does not actually require

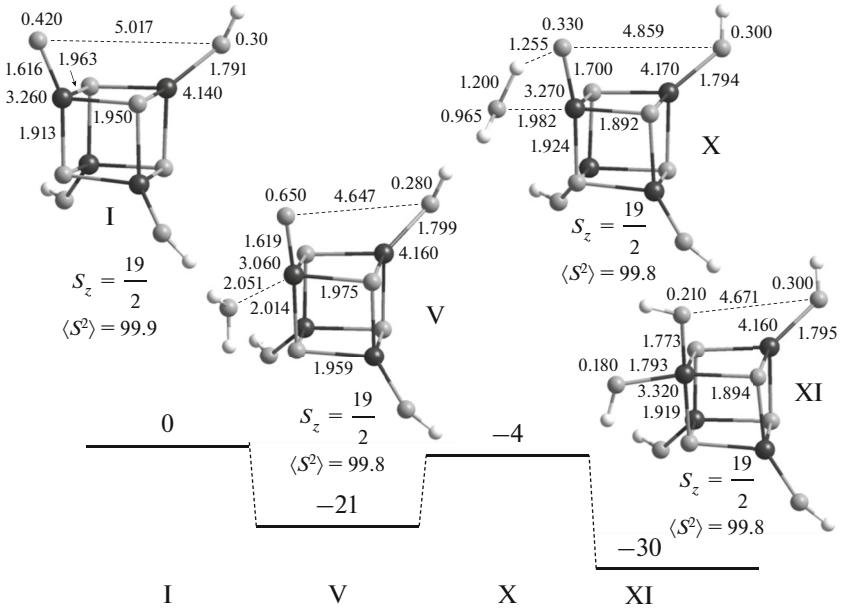

Fig. 8. Formation of two hydroxyl groups at one center under an attack of the water molecule on terminal ferryl oxygen. For designations, see Fig. 7.

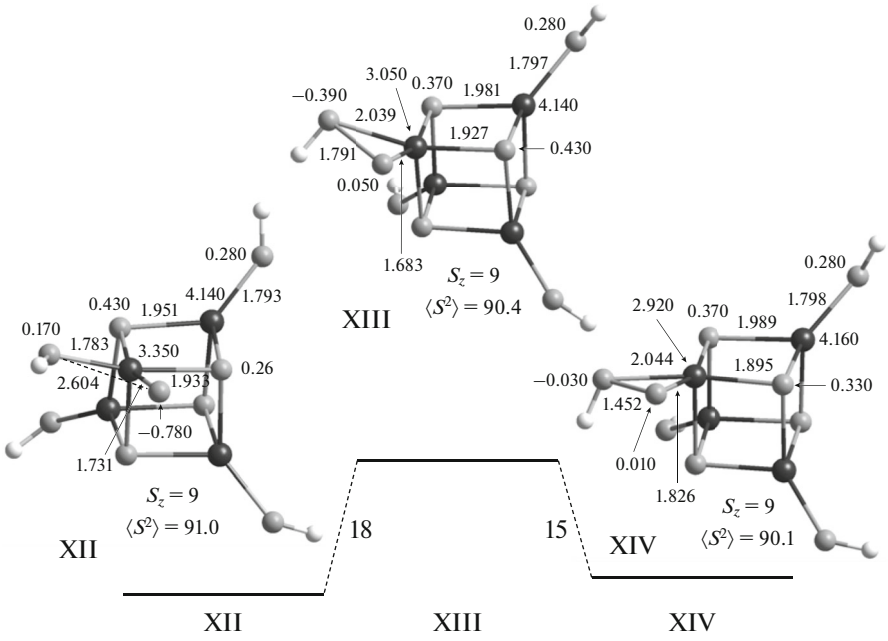

Fig. 9. Formation of hydroperoxide from structure XI in the state S_2 at one center (after the removal of the second electron/proton pair). For designations, see Fig. 7.

activation energy because the transition state is located in an energy scale 4.2 kcal/mol lower than starting complex I. The high stability of hydroxo complex XI, which is 30 kcal/mol more advantageous than starting complex I, is a remarkable fact.

Further, complex XI after the detachment of hydrogen (according to our calculations, 114.0 kcal/mol is required for this process) from an OH group is converted into a complex where oxo and hydroxo ligands are present at one center (structure XII, Fig. 9). Note that the oxo center of this structure is the oxyl radical, which is very highly reactive with respect to the detachment of hydrogen from the C–H bond [52, 53]. Upon association, these ligands overcame a relatively

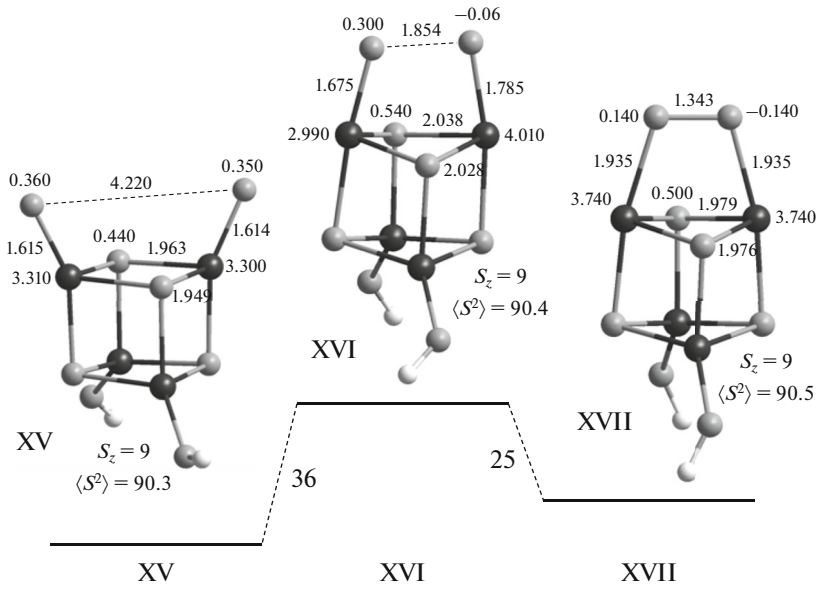

Fig. 10. Designations are the same as in Fig. 7.

low barrier of ~18 kcal/mol to afford the OOH group (structure XIII in Fig. 9). The release of molecular oxygen by this reaction route requires the further substitution of a water molecule for the OOH ligand with the detachment of two electrons and two protons.

Association of Two Ferryl Oxo Centers

This route corresponds to the detachment of two electrons and two protons from the starting system. Figure 10 shows a possible version of the association of two ferryl oxygen centers of a tetramer with parallel spins on the Fe centers. (A distinguishing feature of the ferryl state Fe=O is the same (positive) sign of Mulliken spin density on Fe and O in contrast to the oxyl state $Fe^{III}–O^{\bullet}$, which is characterized by strong spin polarization with a negative density on the oxygen center.) In this case, the height of the energy barrier is sufficiently high (about 36 kcal/mol); this may be due to the reverse transfer of electron density from oxygen to metal with the formation of a peroxo group. Because the spin densities on the interacting atoms of oxygen in the test ferromagnetic tetramer have the same sign, it was hypothesized that the large height of the barrier is related to the Pauli repulsion. To test this hypothesis, the process of oxo center association in an antiferromagnetic state of the dimer $Fe_2O_2(OH)_4$, which possesses two terminal $[FeO]^{2+}$ oxo centers, with antiparallel spins on metals and antiferromagnetic binding in each of them was examined (Fig. 11). Indeed, the direct binding barrier in this model system was found much lower (22 rather than 36 kcal/mol). However, dimer XXIV itself (Fig. 11) with oxyl oxo centers in the starting state is highly excited (energy, 31 kcal/mol) with respect to the ferromagnetic dimer; for this reason, this scenario is improbable.

Introduction of Ferryl Oxygen into the Edge of a Tetramer

This route begins with the addition of the molecule of water to the Fe(IV) center (structure V, Fig. 12), which initiates the incorporation of a ferryl oxo center into the edge of the Fe_4O_4 cube. Energy losses in this route are compensated in an essential measure by the energy of the coordinate bond $Fe–H_2O$ (21 kcal/mol). Two transition states (structures VI and VIII, Fig. 12) were found in this reaction route; however, only structure VIII of them corresponds to a transition state in the process of peroxo group formation because the O–O distance in this structure is considerably shorter (approximately 1.8 Å). As judged from the presence of two relatively short Fe–O bonds, the first of the transient states (VI) corresponds to the formation of an oxo complex with two terminal Fe–O groups. The resulting effective activation energy is relatively small (~12 kcal/mol). Thus, the migration of ferryl oxygen leads to the formation of a peroxo group (with an O–O bond length of ~1.5 Å) in the tetracomplex of iron (structure IX, Fig. 12). The further release of this group in the form of molecular oxygen can occur, for example, through the replacement of the peroxo group by an additional molecule of water with the detachment of three electrons and three protons from the resulting system.

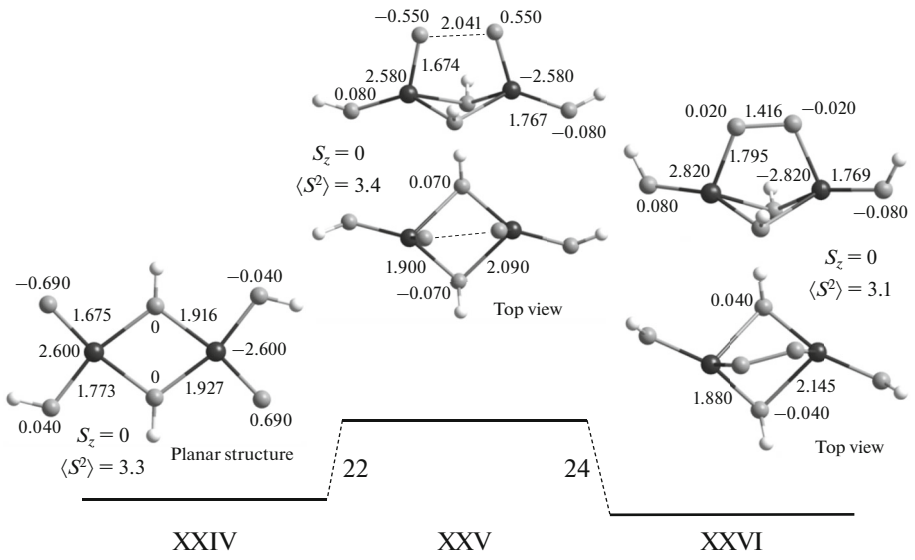

Fig. 11. Direct binding of oxyl centers in the antiferromagnetically bound dimer $Fe_2O_2(OH)_4$. Transition state XXV and product XXVI are depicted in two projections: top and side views. For designations, see Fig. 7.

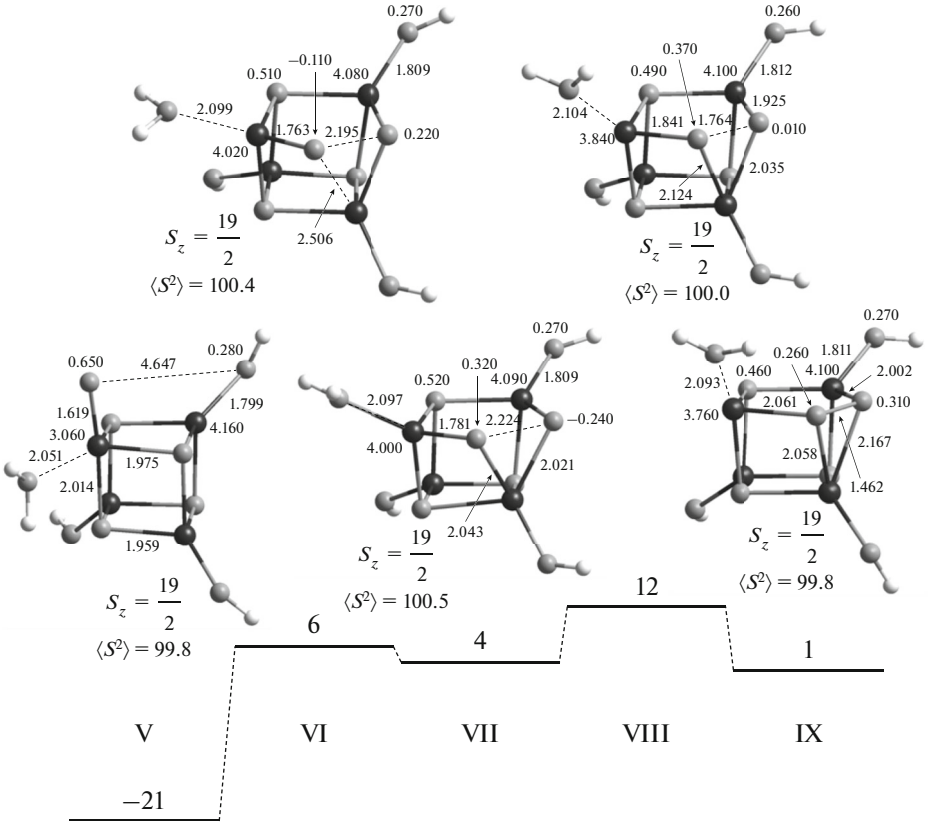

Fig. 12. Introduction of ferryl oxygen FeO into the edge of a tetramer with the formation of a peroxo group from water on iron hydroxide (the tetramer $Fe_4O_4(OH)_4$ in the model) according to the data of B3LYP calculations. The spin projections, the calculated expected value of the squared spin operator, energies (in kcal/mol) relative to a complex with the ferryl group and an isolated molecule of water, bond lengths to within the third decimal digit (in Å), and Mulliken spin densities on the atoms (in au) to within the second decimal digit are given [54]. For designations, see Fig. 7.

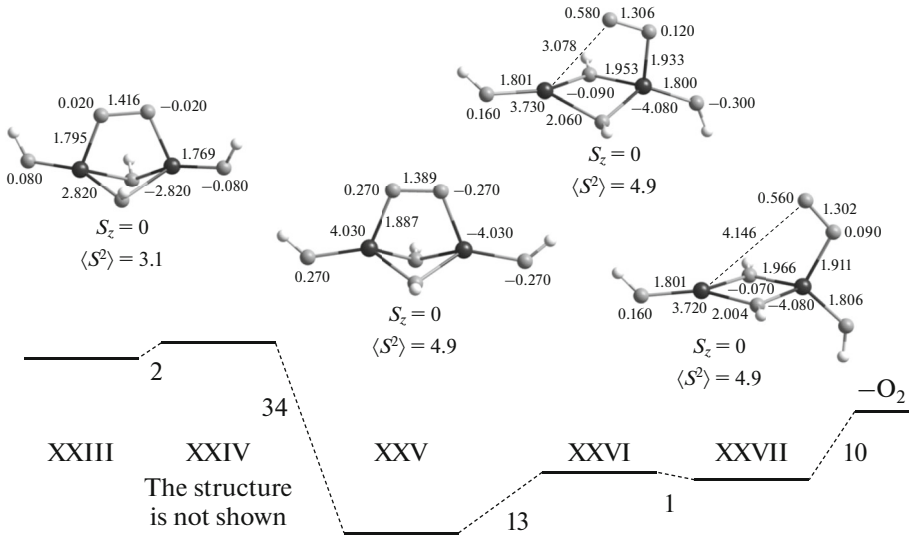

Fig. 13. Yield of molecular oxygen in the dimeric model. For designations, see Fig. 7.

Elimination of Molecular Oxygen

The final structure formed upon the introduction of a ferryl center into the edge of a cube (structure IX, Fig. 12) can be related to a superoxide structure based on the O–O bond length (~1.5 Å). This structure should be converted into a much more stable peroxide structure with a smaller O–O bond length, as this was shown for a dimer (transition from structure XXIII to structure XXV, Fig. 13). The subsequent release of molecular oxygen occurs through a barrier related to the rupture of the coordinate bond of the peroxo group initially with one Fe center (structure XXVI, Fig. 13) and then with the second center. In this case, the released O_2 molecule takes away an effective spin density of ~0.65 au (structure XXVII, Fig. 13). This indicates the formation of the molecule of oxygen in the ground triplet state. Because the spin projection of the entire dimer is 0, the yield of the triplet molecule is compensated by an increase in the negative spin density on one of the Fe centers from −2.82 to −4.08 au for starting structure XXIII and final structure XXVII, respectively (Fig. 13).

The most probable route of the oxidation of water proposed previously [49, 54] is the binding of oxygen of the ferryl group $Fe^{IV}=O$ (which results from the detachment of the first electron and proton from the hydroxyl group by an external oxidant) with the nearest μ_3-oxo center. The effective activation energy of this reaction route is 12 kcal/mol (relative to the initial complex and the water molecule not bound to it), which is close to the activation energy of the rate-determining stage of the overall process of water oxidation characterized (under the assumption that the reaction is unimolecular) by a constant of about 1000 s^{-1}. Three metallic centers directly participate in the process of association according to this route; this is also consistent with the experimental data.

The key processes leading to the formation of a bond between oxygen-containing centers proceed only in the states S_1 and S_2. The introduction of ferryl oxygen into the edge of cubane with the formation of a peroxo group in place of the oxygen apex of cubane indicates that three Fe centers should be present simultaneously. This circumstance justifies the use of cubane as a model of oxygen-releasing center in spite of the absence of a fourth center from iron hydroxides. However, most importantly, this clarifies the reason for the presence of the fourth Mn cation out of the cube in the natural oxygen-releasing chair-like Mn_4CaO_5 center.

Another important advantage of the assumed route of incorporation is the circumstance that, in accordance with it, immediately after the formation of a ferryl center (with the participation of an external oxidant), it "hides" in the edge of a cube and becomes almost inaccessible for an attack of water molecules from solution; this can lead to the protonation of terminal oxygen and stop the oxidation of water.

The formal reaction scheme includes the following key stages: first, proton detachment from the catalyst hydroxo group $[M^{III}–OH]^{2+}$ and the addition of the complex $Ru(bpy)_3^{3+}$

$$[M^{III}–OH]^{2+} + Ru(bpy)_3^{3+} \rightleftarrows [M^{III}–O]^{+} \cdots Ru(bpy)_3^{3+},$$

and the subsequent electron transfer to ruthenium with the formation of an yl group

$$[M^{III}–O]^{+} \cdots Ru(bpy)_3^{3+} \rightarrow [M^{IV}=O]^{2+} + Ru(bpy)_3^{2+}.$$

This process can occur synchronously with proton transfer. In this case, the electron is transferred sepa-

rately from the proton along another orbital channel within the framework of a so-called proton-coupled electron transfer mechanism [55, 56]. The terminal oxygen-containing center is further involved in the following competing reaction routes of the release of molecular oxygen:

(1) association with the hydroxyl group at the same (less probably, at the adjacent) metal center with the formation of hydroperoxide,

(2) association with the adjacent yl oxo center, and

(3) introduction of the yl oxo center into its own μ_3-oxo bridging bond with the formation of a superoxo/peroxo group, in which the O–O bond is formed as a precursor of molecular oxygen.

The results of DFT calculations with the cubane-like cluster of iron atoms indicate that the last route is preferable. In this case, the associates of oxo centers are formed through the oxyl configuration $[Fe^{III}–O^{\bullet}]^{2+}$ of the ferryl group, which manifests itself in transition states and determines the radical-like reactivity of the ferryl center, for example, in the detachment of hydrogen from methane [52, 53]. Note that, in addition to the above routes, in principle, there is a route of the direct dissociation of the water molecule from the environment at the ferryl center with the formation of $H^{\bullet}$ or $OH^{\bullet}$ free radicals:

$$[M^{IV}=O]^{2+} + H_2O \rightarrow \begin{matrix}[M^{III}–OOH]^{2+} + H^{\bullet} \\ \searrow \\ [M^{III}–OH]^{2+} + OH^{\bullet}.\end{matrix} \quad \text{(XXV)}$$

We do not consider this route because there are experimental data on the critical importance of a distance between metal atoms for the reaction of water oxidation [35], which are indicative of the occurrence of the process at the centers containing at least two metal atoms.

CONCLUSIONS

The review of the results of early studies directed toward the development of artificial catalysts for water oxidation to oxygen by one-electron oxidants primarily conducted at the Boreskov Institute of Catalysis, Siberian Branch of the Russian Academy of Sciences in 1980–2000 indicates on noticeable achievements, which remain of considerable current interest. This is true of the development of highly active catalysts for the above process based on the simple hydroxo compounds of some transition metals and the experimental and theoretical studies of the mechanism of water oxidation by one-electron oxidizing agents.

The experimentally evidenced and substantiated by quantum-chemical calculations conclusion that compounds capable of catalyzing the oxidation of water should meet a number of requirements is most important. First, it is necessary for the functional active center of these compounds to be a hydroxide containing metal atoms that can sustainably exist in at least three sequential oxidation states (for example, these are II, III, and IV for Mn, Fe, and Co; III, IV, and V for Ru; or I, II, and III for Cu). Second, the active center of the catalyst should possess free coordination sites or labile ligands, which can be easily replaced by water or OH groups. Third, the ligands used for stabilizing the active center should not be strong electron donors or acceptors because otherwise the oxidation of the ligands instead of water becomes preferable or a decrease in the electron density on metal atoms and, as a result, a decrease in the oxidation potential of the catalyst accompanied by a decrease in the acidity of the coordinated OH group or H_2O molecule occur. Fourth, the compounds should be capable of forming di- and polynuclear structures of the μ-hydroxo or μ-oxo type. In this case, the circumstance that a metal–metal distance in the catalyst directly affects the height of an energy barrier in the reaction of O–O bond formation is of importance.

All of these requirements can be satisfied using both free and stabilized transition metal hydroxo compounds with controlled structural parameters. In spite of significant differences in the structures of artificial catalysts for the oxidation of water and the natural calcium–manganese cluster of the oxygen-releasing complex of the photosystem II of green plants, the mechanisms of action of both catalytic systems have much in common. Primarily, this is true of the polynuclear structure of complexes and hydroxo compounds, which can perform the accumulation of one-electron oxidizing equivalents and, thus, carry out not only two-electron but also four-electron oxidation processes. In this case, it is significant that these processes cannot be necessarily reduced to the synchronous transfer of several electrons, but they include the formation of intermediates with O–O bonds. The initial ratios between the oxidation states of manganese in the active centers of catalysts, which are very similar for the most active artificial Mn-containing hydroxo compounds and the natural oxygen-releasing complex, namely, Mn(III) : Mn(IV) = 3 : 1, have engaged our attention.

The revealed special features of the catalysts of water oxidation indicate that it is reasonable to develop colloidal catalysts and catalysts based on the hydroxo compounds of Mn, Fe, Co, and Cu supported onto solid carriers. Microheterogeneous systems are promising from the point of view of their use both for studying the mechanism of water oxidation and for further immobilization, for example, on lipid membranes in order to develop artificial molecular photocatalytic systems that imitate the natural photosynthesis of green plants. The development of the catalysts stabilized on the surface of traditional oxide carriers is promising because the size and structure of active centers can be finely regulated and the electron structure of nanosized hydroxo particles can be controllably changed by their interaction with the carrier surface in

order to improve the characteristics of the catalysts. It is also obvious that the studies of the reaction mechanism by both kinetic and quantum-chemical methods should be continued because this will make possible to pass from a current almost combinatory approach to the target-oriented design of catalysts with specified properties.

ACKNOWLEDGMENTS

This work was supported by the Russian Foundation for Basic Research (grant no. 15-29-01275).

REFERENCES

1. Larkum, A.W.D., *Curr. Opin. Biotec.*, 2010 vol. 21, p. 271.
2. *BP Statistical Review of World Energy*, 2016.
3. Kunin, E.V., *Logika sluchaya. O prirode i proiskhozhdenii biologicheskoi evolyutsii* (The logic of the case. On the nature and origin of biological evolution), Moscow: Tsentrpoligraf, 2014.
4. Rappaport, F., Guergova-Kuras, M., Nixon, P.J., Diner, B.A., and Lavergne, J., *Biochemistry*, 2002, vol. 41, p. 8518.
5. Umena, Y., Kawakami, K., Shen, J.-R., and Kamiya, N., *Nature*, 2011, vol. 473, p. 55.
6. Kok, B., Forbush, B., and McGloin, M., *Photochem. Photobiol.*, 1970, vol. 11, p. 457.
7. Suga, M., Akita, F., Sugahara, M., Kubo, M., Nakajima, Y., Nakane, T., Yamashita, K., Umena, Y., Nakabayashi, M., Yamane, T., Nakano, T., Suzuki, M., Masuda, T., Inoue, S., Kimura, T., Nomura, T., Yonekura, S., Yu, L.-J., Sakamoto, T., Motomura, T., Chen, J.-H., Kato, Y., Noguchi, T., Tono, K., Joti, Y., Kameshima, T., Hatsui, T., Nango, E., Tanaka, R., Naitow, H., Matsuura, Y., Yamashita, A., Yamamoto, M., Nureki, O., Yabashi, M., Ishikawa, T., Iwata, S., and Shen, J.-R., *Nature*, 2017, vol. 543, p. 131.
8. Elizarova, G.L. and Parmon, V.N., *Fotokataliticheskoe preobrazovanie solnechnoi energii* (Photocatalytic transformation of sun energy), part 2, Novosibirsk: Nauka, 1985.
9. Mills, A., *Chem. Soc. Rev.*, 1989, vol. 18, p. 285.
10. Ruttinger, W. and Dismukes, C.G., *Chem. Rev.*, 1997, vol. 97, no. 1, p. 1.
11. Liu, X. and Wang, F., *Coord. Chem. Rev.*, 2012, vol. 256, nos 11–12, p. 1115.
12. Yamazaki, H., Shouji, A., Kajita, M., and Yagi, M., *Coord. Chem. Rev.*, 2010, vol. 254, nos. 21–22, p. 2483.
13. Liu, X., Inagaki, S., and Gong, J., *Angew. Chem. Int. Ed. Engl.*, 2016, vol. 55, p. 14924.
14. Collin, J.P. and Sauvage, J.P., *Inorg. Chem.*, 1986, vol. 25, p. 135.
15. Hunter, B.M., Gray, H.B., and Muller, A.M., *Chem. Rev.*, 2016, vol. 116, p. 14120.
16. Najafpour, M.M., Ghobadi, M.Z., Haghighi, B., Tomo, T., Shen, J.R., and Allakhverdiev, S.I., *BBA–Bioenergetics*, 2015, vol. 1847, no. Iss. 2, p. 294.
17. Zhou, H., Yan, R., Zhang, D., and Fan, T., *Chem.-Eur. J.*, 2016, vol. 22, p. 1.
18. Yamamoto, M. and Tanaka, K., ChemPlusChem, 2016, vol. 81, p. 1.
19. Sartorel, A., Carraro, M., Scorrano, G., Zorzi, R.D., Geremia, S., McDaniel, N.D., Bernhard, S., and Bonchio, M., *J. Am. Chem. Soc.*, 2008, vol. 130, no. 15, p. 5006.
20. Elizarova, G.L., Matvienko, L.G., Lozhkina, N.V., Maizlish, V.E., and Parmon, V.N., *React. Kinet. Catal. Lett.*, 1981, vol. 16, nos. 2–3, p. 285.
21. Elizarova, G.L., Matvienko, L.G., Lozhkina, N.V., Parmon, V.N., and Zamaraev, K.I., *React. Kinet. Catal. Lett.*, 1981, vol. 16, nos. 2-3, p. 191.
22. Elizarova, G.L., Zhidomirov, G.M., and Parmon, V.N., *Catal. Today*, 2000, vol. 58, no. 2, p. 71.
23. Parmon, V.N., Elizarova, G.L., Matvienko, L.G., Lozhkina, N.V., and Maizlish, V.E., *Izv. Akad. Nauk SSSR, Ser. Khim.*, 1984, vol. 8, p. 1735.
24. Elizarova, G.L., Matvienko, L.G., Parmon, V.N., and Zamaraev, K.I., *Dokl. Akad. Nauk SSSR*, 1979, vol. 249, no. 4, p. 863.
25. Zoski, C.G., *Handbook of Electrochemistry*, Boston: Elsevier, 2007.
26. Aiso, K., Takeuchi, R., Masaki, T., Chandra, D., Saito, K., Yui, T., and Yagi, M., *ChemSusChem*, 2017, vol. 10, p. 687.
27. Friebel, D., Louie, M.W., Bajdich, M., Sanwald, K.E., Cai, Y., Wise, A.M., Cheng, M.-J., Sokaras, D., Weng, T.-C., Alonso-Mori, R., Davis, R.C., Bargar, J.R., Norskov, J.K., Nilsson, A., and Bell, A.T., *J. Am. Chem. Soc.*, 2015, vol. 137, p. 1305.
28. Singh, A., Fekete, M., Gengenbach, T., Simonov, A.N., Hocking, R.K., Chang, S.L.Y., Rothmann, M., Powar, S., Fu, D., Hu, Z., Wu, Q., Cheng, Y.-B., Bach, U., and Spiccia, L., *ChemSusChem*, 2015, vol. 8, p. 4266.
29. Singh Gujral, S., Simonov, A.N., Fang, X.-Y., Higashi, M., Gengenbach, T., Abe, R., and Spiccia, L., *Catal. Sci. Technol.*, 2016, vol. 6, no. 11, p. 3745.
30. Elizarova, G.L., Matvienko, L.G., Lozhkina, N.V., Parmon, V.N., and Moroz, E.M., *Izv. Sib. Otd. Akad. Nauk SSSR, Ser. Khim.*, 1990, vol. 3, p. 86.
31. Elizarova, G.L., Matvienko, L.G., and Parmon, V.N., *J. Mol. Catal.*, 1987, vol. 43, p. 171.
32. Elizarova, G.L., Matvienko, L.G., Taran, O.P., Parmon, V.N., and Kolomiichuk, V.N., *Kinet. Katal.*, 1992, vol. 33, no. 4, p. 898.
33. Young, I.D., Ibrahim, M., Chatterjee, R., Gul, S., Fuller, F.D., Koroidov, S., Brewster, A.S., Tran, R., Alonso-Mori, R., Kroll, T., Michels-Clark, T., Laksmono, H., Sierra, R.G., Stan, C.A., Hussein, R., Zhang, M., Douthit, L., Kubin, M., Lichtenberg, C., Pham, L.V., Nilsson, H., Cheah, M.H., Shevela, D., Saracini, C., and Bean, M.A., *Nature*, 2016, vol. 540, p. 453.
34. Elizarova, G.L., Matvienko, L.G., Pestunova, O.P., and Parmon, V.N., *Kinet. Katal.*, 1994, vol. 35, no. 3, p. 362.
35. Elizarova, G.L., Matvienko, L.G., Kuznetsov, V.L., Kochubey, D.I., and Parmon, V.N., *J. Mol. Catal. A. Chem.*, 1995, vol. 103, p. 43.

36. Elizarova, G.L., Zhidomirov, G.M., and Parmon, V.N., *Catal. Today*, 2000, vol. 58, p. 71.
37. Chikunov, A.S., Taran, O.P., and Parmon, V.N., *Proc. 21 Int. Conf. on Photochemical Conversation and Storage of Solar Energy,* St. Peterburg: SPBU, 2016, p. 54.
38. Elizarova, G.L., Gerasimov, O.V., Matvienko, L.G., Lozhkina, N.V., and Parmon, V.N., *Izv. Sib. Otd. Akad. Nauk SSSR, Ser. Khim.*, 1990, vol. 3, p. 94.
39. Pestunova, O.P., Elizarova, G.L., Gerasimov, O.V., and Parmon, V.N., *Kinet. Katal.*, 2000, vol. 41, no. 3, p. 375.
40. Khannanov, N.K., Khramov, A.V., Moravskii, A.P., and Shafirovich, V.Ya., *Kinet. Katal.*, 1983, vol. 24, no. 4, p. 858.
41. Pendlebury, S.R., Barroso, M., Cowan, A.J., Sivula, K., Tang, J., Gratzel, M., Klug, D., and Durrant, J.R., *Chem. Commun.*, 2011, vol. 47, no. 2, p. 716.
42. Barroso, M., Pendlebury, S.R., Cowan, A.J., and Durrant, J.R., *Chem. Sci.*, 2013, vol. 4, no. 7, p. 2724.
43. Young, K.M.H., Klahr, B.M., Zandi, O., and Hamann, T.W., *Catal. Sci. Technol.*, 2013, vol. 3, no. 7, p. 1660.
44. Cristensen, P.A., Harriman, A., Porter, G., and Neta, P., *J. Chem. Soc. Faraday Trans. II*, 1984, vol. 80, p. 1451.
45. Gerasimov, O.V., Lymar, S.V., and Parmon, V.N., *J. Photochem. Photobiol. A. Chem.*, 1991, vol. 56, p. 275.
46. Gerasimov, O.V., Lymar, S.V., Tsvetkov, T.M., and Parmon, V.N., *React. Kinet. Catal. Lett.*, 1987, vol. 36, p. 145.
47. Li, X. and Siegbahn, P.E.M., *J. Am. Chem. Soc.*, 2013, vol. 135, p. 13804.
48. Kok, B., Forbush, B., and Mcgloin, M., *Photochem. Photobiol.*, 1970, vol. 11, no. 6, p. 457.
49. Filatov, M.J., Elizarova, G.L., Gerasimov, O.V., Zhidomirov, G.M., and Parmon, V.N., *J. Mol. Catal.*, 1994, vol. 91, p. 71.
50. Wang, L.-P. and Van Voorhis, T., *J. Phys. Chem. Lett. Am. Chem. Soc.*, 2011, vol. 2, no. 17, p. 2200.
51. Mavros, M.G., Tsuchimochi, T., Kowalchuk, T., Mclsaac, A., Wang, L.-P., and Voorhis, T.V., *Inorg. Chem. Am. Chem. Soc.*, 2014, vol. 53, no. 13, p. 6386.
52. Shubin, A.A., Ruzankin, S.P., Zilberberg, I.L., and Parmon, V.N., *Chem. Phys. Lett.*, 2015, vol. 640, p. 94.
53. Zilberberg, I.L., Shubin, A.A., Ruzankin, S.P., Kovalskii, V.Y., Ovchinnikov, D.A., and Parmon, V.N., *AIP Conf. Proc.*, 2016, p. 20027.
54. Shubin, A.A., Ruzankin, S.P., Zilberberg, I.L., Taran, O.P., and Parmon, V.N., *Chem. Phys. Lett.*, 2015, vol. 619, p. 126.
55. Liao, R.-Z. and Siegbahn, P.E.M., *J. Photochem. Photobiol.*, 2015, vol. 152, p. 162.
56. Dietl, N., Schlangen, M., and Schwarz, H., *Angew. Chem. Int. Ed. Engl.*, 2012, vol. 51, p. 5544.

Translated by V. Makhlyarchuk